Importance of interaural time difference in coding the azimuth in the central nucleus of the inferior colliculus in the barn owl (*Tyto alba*)

Von der Fakultät für Mathematik, Informatik und Naturwissenschaften
-Fachbereich I-
der Rheinisch-Westfälischen Technischen Hochschule Aachen
zur Erlangung des akademischen Grades
eines Diplom Biologen
genehmigte Diplomarbeit

vorgelegt von
Peter Bremen
aus Stolberg (Rhld.)

Berichter: Universitätsprofessor Dr. rer. nat. H. Wagner
Privatdozent Dr. rer. nat. H. Luksch

Contents

Chapter 1

General introduction

Humans are said to mainly rely on their eyes when mastering daily life. Audition seems to play only a minor role in orienting. However, the visual and auditory system are deeply entangled (Heffner et al. 1999): While the visual system scans the frontal space and is restrained by the eye and head movement, the auditory system constantly surveys the whole space around us and elicits head and body turns to shift the visual attention towards the strange noise coming from the rear. The auditory system is even able to localize a sound source precisely within one degree. What are the basic principles underlying sound localization?

According to Krogh's principle[1] it is reasonable to study a specialist in the field of sound localization to solve this question. Hence, nocturnal predators like barn owls (*Tyto alba*, hereafter referred to as the owl) that mostly rely on their sense of hearing to localize their prey, are established animal models in auditory research (Wagner 1995).

However, one major difference becomes evident when comparing the auditory and the visual system that leads to a different representation and computation of auditory space in the brain. While neighbouring visual objects are represented adjacent to each other in the retina creating a retinotopic map of space, no map of auditory space is found in the cochlea. Instead the frequencies contained in the sound

---

[1] Krogh's principle states that for all possible research questions there should be at least one animal adequately suited to solve this special question. E.g. the giant axon of the squid made the elucidation of the action potential by Hodgkin and Huxley possible.

are represented on a tonotopic or frequency map along the basilar membrane. This leads to the necessity to compute a map of space in the ascending auditory pathway (Wagner 2004).

To compute the sound source's location in space, the interaural time difference (ITD) and interaural level difference (ILD) are analyzed as well as monaural cues resulting mainly from the owl's characteristic facial ruff and preaural flaps. The ITD arises from a difference in the length of the path on which the sound waves travel towards the right and the left ears. ITDs are sufficient to elicit an azimuthal head turn response in the owl (Moiseff 1989; Poganiatz et al. 2001). The level differences arise due to the amount of attenuation and amplification between each ear and elicit elevational head turns in owls (Moiseff 1989). Monaural cues are attributable to the individual filter characteristics of the facial ruff. One of their roles is to aid avoiding front-back confusions.

To study the contribution of every single cue in detail, it is important to be able to vary each parameter separately. The only method offering such a control is the virtual acoustic space (VAS) technique, which was employed in this thesis to investigate the influence of ITD on coding azimuth in the owl's midbrain. The thesis is organized in four chapters, each organized like a manuscript. In this chapter a general discussion of the advantages of the owl as an animal model, the VAS technique and the aim of this thesis will be given. Chapter 2 describes the VAS technique in greater detail with special emphasis on the calculation of ITD, ILD and HRTFs. In chapter 3 the auditory pathway up to the midbrain nuclei, the stimulus paradigm used and the electrophysiological experiments are presented. The thesis is concluded with a general discussion in chapter 4. Every chapter closes with a complete list of references cited in the respective chapter.

1.1 Aim and organization of this thesis

Is ITD the only cue necessary to code azimuth? Up to now this has only been shown on a behavioural level (Knudsen and Konishi 1979; Knudsen and Knudsen 1986), indirectly via lesion studies (Wagner 1993) and in part on an electrophysiological level in space-specific midbrain neurons (Olsen et al. 1989). However, in all of these studies stimuli contained only one binaural cue. So far only one behavioural study employed the VAS technique to investigate the influence of ITD while other natural cues are present (Poganiatz et al. 2001).

Therefore, the aim of the present thesis is to investigate – on an electrophysiological level – if ITD is the only parameter that influences the coding of azimuth. Tuning properties of neurons in the core of the central nucleus of the inferior colliculus (ICc-core) of the owl were recorded to test this hypothesis, because their response varies with ITD, but not with ILD.

1.2 Animal model

As a nocturnal predator the owl is specialized to localize and catch its prey in total darkness using mostly its excellent sense of hearing (Payne 1962, 1971; Konishi 1973). One of the typical hunting strategies of owls is to sit motionless on an elevated position before striking and to turn the head towards the location of sounds caused by a potential prey (Brandt and Seebass 1994). This behaviour is due to the inability of the owl to move its eyes in the eye-sockets (Steinbach and Money 1973) and to move its external ears. Under laboratory conditions this head turning behaviour is easily measured (Wagner 1995), in contrast to the orienting behaviour of monkeys, who move their eyes and head (Zwiers et al. 2004), and cats, which in addition use their pinnae to localize sounds (Middlebrooks and Knudsen 1987).

The possibility to conduct electrophysiological and anatomical experiments with owls, in recent years led to the understanding of the basic stations of the auditory pathway from the cochlear nuclei via the midbrain to the forebrain (for details see Chapter 3). Together with the fact that owls are easily kept in aviaries and bread the whole year, these animals are the ideal model animals to study the basic principles underlying the information processing in the auditory system.

1.3 Virtual acoustic space

Classical psychophysical and neurophysiological studies employed two techniques to deliver the stimulus to the subject. The simplest approach is to emit the sound from loudspeakers positioned around the head of the subject. The stimuli in these so-called free-field studies are filtered in a natural way by the subject’s torso, head (owls: in addition facial ruff) and ear, giving rise to various spatial cues depending on the position of the sound source. Employing this method the head turning behaviour of owls towards sounds could be measured (Knudsen et al. 1979a; Knudsen and Konishi 1979b; Knudsen and Knudsen 1986). This technique is closest to the natural condition but an independent manipulation of the stimulus for each ear is impossible.

The presentation of sounds via earphones allows such dichotic stimulation. Thus, it is possible to investigate the influence of ITDs and ILDs on behavioural or neuronal responses. However, the presentation of sounds over headphones leads to a lateralization (i.e. sounds appear to come from the right or left). This is due to the lack of filtering by the external ear: The sound is perceived as if it is emitted inside the head. The use of this method led to the discovery that in the owl ITD is the main parameter used for the azimuthal localization while ILD on the other hand is used for elevational localization of a sound (Moiseff 1989; Wagner 1991; Poganiatz 2001).

With the advent of sophisticated signal processing hard- and software, a hybrid of these two techniques the so-called virtual acoustic space (VAS) stimulation became possible. A faithful replication of the subject’s filtering properties is made by recording sounds emitted in free-field with probe microphones inserted into the ear canal. This data is then incorporated as digital filters into the signal presented via the headphones. Thus, the signal becomes externalized, i.e. the sound is perceived as if presented from a real source in space. The accuracy of localization is comparable to the free-field situation (humans: Whightman and Kistler 1989a, b; owl: Poganiatz 2001). The VAS technique overcomes the limitations of free-field and headphone studies. On the one hand it is possible to manipulate the stimulus’ features for each ear independently, while on the other hand all natural localization cues are present.

1.4 References

Brandt T and Seebass C (1994) Die Schleiereule. Aula-Verlag, Wiesbaden

Heffner RS, Koay G, Heffner HE (1999) Sound localization in an Old-World fruit bat (*Rousettus aegyptiacus*): acuity, use of binaural cues, and relationship to vision. *J. Comp. Psychol.* 113: 297-306

Knudsen EI and Knudsen PF (1986) The sensitive period for auditory localization in the barn owl is limited by age not by experience. *J. Neuroscience* 6: 1918-1924

Knudsen EI, Blasdel GG, Konishi M (1979a) Sound localization by the barn owl (*Tyto alba*) measured with the search coil technique. *J. Comp. Physiol. A* 133: 11-11

Knudsen EI and Konishi M (1979b) Mechanisms of sound localization in the barn owl (*Tyto alba*). *J. Comp. Physiol. A* 133: 12-21

Konishi M (1973) How the Owl tracks its Prey. *Am. Sci.* 61: 414-424

Middlebrooks JC and Knudsen EI (1987) Changes in the external ear position modify the spatial tuning of auditory units in the cat's superior colliculus. *J. Neurophysiol.* 57: 672-687

Moiseff A (1989) Bi-coordinate Sound Localization by the Barn Owl. *J. Comp. Physiol. A* 164: 637-644

Payne RS (1962) How the barn owl locates prey by hearing. *The Living Bird, First Annual of the Cornel Laboratory of Ornithology* 151-159

Payne RS (1971) Acoustic location of prey by barn owls (*Tyto alba*). *J. Exp. Biol.* 54: 535-573

Poganiatz I (2000) Sound-localization in barn owls – Experiments with virtual space stimuli – *PhD-Thesis at the Reihnisch-Westfälische Technische Hochschule Aachen*

Poganiatz I, Nelken I, Wagner H (2001) Sound-localization experiments with barn owls in virtual space: influence of interaural time difference on head-turning behavior. *J. Assoc. Res. Otolaryngol.* 2: 1-21

Steinbach MJ and Money KE (1973) Eye movements of the owl. *Vision Res.* 13: 889-891

Olsen JF, Knudsen EI, Esterly SD (1989) Neural maps of interaural time and intensity differences in the optic tectum of the barn owl. *J. Neurosci.* 9: 2591-2605

Wagner H (1991) A temporal window for lateralization of interaural time difference by the barn owls. *J. Comp. Physiol. A* 169: 281-289

Wagner H (1993) Sound-localization deficits induced by lesions in the barn owl's space map. *J. Neuroscience* 13: 371-386

Wagner H (1995) Sound-localization experiments in owls. In: Klump GM, Dooling RJ, Fay RR, Stebbins WC (eds) *Methods in comperative Psychoacoustics* Birkhäuser Verlag Basel/Switzerland

Wagner H (2004) A comparison of neural computations underlying stereo vision and sound localization. *J. Physiol.* 98: 135-145

Wightman FL and Kistler DJ (1989a) Headphone simulation of free-field listening I. Stimulus synthesis. *J. Acoust. Soc. Am.* 85: 858-867

Wightman FL and Kistler DJ (1989b) Headphone simulation of free-field listening I. Psychophysical validation. *J. Acoust. Soc. Am.* 85: 868-878

Zwiers MP, Versnel H, van Opstal AJ (2004) Involvement of Monkey Inferior Colliculus in Spatial Hearing. *J. Neurosci.* 24: 4145-4156

Chapter 2

Virtual acoustic space (VAS)

2.1 Introduction

2.1.1 General remarks

The main cues for sound localization are interaural differences in time of arrival (ITD) and level (ILD). In addition to this, monaural cues due to the filtering characteristics of the torso, head (owls: facial ruff) and pinnae lead to a frequency and space-specific filtering of the incoming sound waves. This gives additional cues to locate the sound source (Yost and Dye 1997). The filtering characteristics of the physical shape of the ears can be measured using careful measurement techniques. The incorporation of these filters, so called head-related transfer functions (HRTF), into stimuli presented over headphones lead to an externalized percept. That is, the listener experiences a virtual free-field situation (Wightman and Kistler 1989a, b). Such an impression is referred to as virtual acoustic space, or VAS for short.

VAS has two major advantages when compared with non-virtual dichotic stimulation. HRTFs simulate a free-field situation evoking a spatial percept, containing all natural spatial cues available for sound localization. At the same time a separate manipulation of each cue is possible. Nevertheless, since for each position in space one pair of filters must be sampled, the preparations before the experiment are more time consuming. A typical recording session as described in this thesis lasts for 4 to 5 hours depending on the sampling resolution (this study: 10° for azimuth and elevation). During the recording the animal needs to be anaesthetized.

In addition to this, the VAS technique is not applicable for freely behaving animals that are able to move their ears, such as cats and monkeys. Pinnae movements dynamically change the filtering characteristics of the ears relative to the head and hence the properties of the HRTFs. In these species VAS studies are only possible when (1) HRTFs can be updated on-line under a given position of the pinnea or when (2) the pinnea are immobilized, as is the case in anesthetized animals limiting its use mostly to electrophysiological questions.

2.1.2 Theory

The main assumption underlying the measurement of HRTFs is the linearity of the system. Physical phenomena like reflection, shadowing, interference and resonance that occur at the torso, head (owls: facial ruff) and pinnae (owls: preaural flaps) in linear system theory can be described by the convolution integral:

$$y(t) = \int_{-\infty}^{\infty} h_{sys}(\tau)x(t-\tau)d\tau \qquad \text{(Eq. 2.1)}$$

with x(t) as the input at the time t, y(t) as the output and $h_{sys}(t)$ as the so-called impulse response (IR) of the system, which completely describes a linear system. The convolution of two functions in the time domain is equivalent to the multiplication of the Fourier transforms (FTs) in the frequency domain (convolution theorem):

$$Y(f) = H(f) \cdot X(f) \qquad \text{(Eq. 2.2)}$$

The upper-case letters denote the FTs of the functions symbolized by the lower-case letters in Eq. 2.1. Accordingly, H(f) is the FTs of $h_{sys}(t)$ and is called the transfer function of the system.

2.2 Methods

Head-Related Impulse Responses (HRIRs) of three living owls, J, O and S, were measured. A typical recording session lasted about 4-5 hours plus 1-2 hours for surgery and preparation before the measurement. All experiments were carried out in accordance with German law and the NIH guidelines for the care and use of laboratory animals and were approved by the Regierungspräsidium Köln.

2.2.1 Measurement of HRIRs

Birds were anesthetized with Valium (Diazepam, 1 mg/kg/h; Merckle GmbH, Blaubeuren) and Ketamin (20 mg/kg/h; Sanofi-CEVA GmbH, Düsseldorf) and wrapped into a jacket. Before the measurement a metal post was cemented to the skull of each bird as described in Wagner (1993). This treatment allowed fixing the head during the recording and experiments to a constant position. The animal was then placed in a sound-attenuating chamber (2.4 m * 2.1 m * 2.7 m, IAC 403A, Industrial Acoustics, Niederkrüchten, Germany; lined with pyramidal foam). The metal post was screwed to a metal holder on a holding device, situated in the centre of a movable semi-circular hoop mounted with a loudspeaker (Macaudio ML-103E, 2-12 kHz: flat within ±3 dB). To stabilize the owl, the body was fixed with tape to the holding device (Poganiatz 2000).

A Sennheiser KE 4-211-2 microphone with a 4 cm long plastic tube (outer diameter 1.4 mm, inner diameter 1.2 mm, length 25 mm) was positioned 15 mm inside the 17 mm long ear canal of each ear. To allow a correct placement, the plastic tubes were marked with a scale leading to variability in position of about ±1 mm (Poganiatz 2000). This reduced the risk of damaging the eardrum without at the same time losing directional information (Keller 1998).

To measure the IRs a frequency sweep (20 Hz to 16 kHz logarithmically rising, 500 ms duration, 5 ms rise/fall time, 5 repetitions per position) was used. They were created by a DA1 (Tucker Davis Technologies, Gainesville) amplified by a HiFi-amplifier (Yamaha AX-590) and emitted by the single loudspeaker. The speaker was mounted on the semi-circular vertical hoop at a distance of 95 cm from the centre of the owl's head and could be moved in azimuth and elevation. The recorded microphone signals were preamplified by custom-build amplifiers, low-pass filtered (Tucker Davis Technologies FT6, cut-off frequency 20 kHz) and digitized by an AP2 computer board (Tucker Davis Technologies; sampling rate 100 kHz, recording length: 510 ms).

A spherical coordinate system with its origin in the centre of the owl's head (azimuth: 0 °; elevation: 0°) was used to describe the positions in space (Poganiatz 2000). Azimuth (ϕ) was defined as the horizontal deviation from the midsaggital plane with positive values denoting the right side and negative ones the left side. Elevation (θ) was described as the vertical deviation from the horizontal plane through the owl's eyes. The upper hemifield was denoted with positive, the lower with negative values. In total 460 positions in space were recorded (ϕ: -160° to 160°; θ: -70° to 70°; resolution 10°) with five repetitions at each position. In the subsequent analysis these repeated recordings were averaged. Recordings varying more than one standard deviation were discarded before averaging.

Three types of measurement were conducted. In the free-field to eardrum recording the movable speaker was used for stimulus presentation, yielding the transfer function $y_0(t)$. The first reference measurement $y_1(t)$ was made before the owl was fixed to the holding device. The microphones were aligned straight ahead in the centre of the hoop and the speaker delivered the sweep. This measurement was needed for the calculation of the HRTFs. The second reference measurement $y_2(t)$ was used to calculate the HRIRs for stimulation via earphones and was conducted at the end of a recording session with the owl still fixed to the holding device. For this measurement the earphones (SONY MDR-E831LP) later to be used in the electrophysiological experiments were placed in front of the owl's ear canals and used for stimulus presentation.

Since one experiment lasted for 6-7 hours recordings were repeatedly interrupted to maintain anaesthesia by the administration of the required substances. These interruptions did not lead to a statistically significant error in the recording results (Poganiatz 2000).

2.2.2 Calculation of HRTFs

The measured HRIRs are a convolution of the transfer functions of the loudspeaker l(t), the facial ruff, ear flaps and the ear canal h(t) and the microphone m(t) with the input $x_0(t)$ as described by the following scheme for one ear:

$$x_0(t) \rightarrow l(t) \rightarrow h(t) \rightarrow m(t) \rightarrow y_0(t)$$

In the frequency domain this can be expressed as:

$$X_0(f) \rightarrow L(f) \rightarrow H_{\phi\theta}(f) \rightarrow M(f) \rightarrow Y_0(f)$$

with $X_0(f)$ and $Y_0(f)$ being the FTs of the input and output, L(f) and M(f) the FTs of l(t) and m(t) and $H_{\phi\theta}(f)$ the free-field-to-eardrum transfer function of one ear for azimuth = ϕ and elevation = θ. Applying the convolution theorem this yields:

$$Y_0(f) = L(f) \cdot H_{\phi\theta}(f) \cdot M(f) \cdot X_0(f) \qquad \text{(Eq. 2.3)}$$

Analogous considerations lead to:

$$Y_1(f) = L(f) \cdot M(f) \cdot X_0(f) \qquad \text{(Eq. 2.4)}$$

for the reference measurement $y_1(t)$ done without the owl. The division of Y_0 and Y_1 obtains the HRTFs:

$$H_{\phi\theta}(f) = \frac{Y_0(f)}{Y_1(f)} \qquad \text{(Eq. 2.5)}$$

This calculation was done for all measured positions in space for both ears. The HRTFs were filtered with a bandpass filter from 2-12 kHz (butterworth, order 16) to minimize effects of frequencies not necessary for sound localization. For subsequent analysis the amplitude ($|H_{\phi\theta}|$) and the phase spectrum ($\arctan(Im(H_{\phi\theta}/Real(H_{\phi\theta})))$) from the complex function $H_{\phi\theta}$ was calculated.

2.2.4 Calculation of HRIRs for virtual acoustic stimuli

For the calculation of the HRIRs the second reference measurement is needed (Wightman and Kistler 1989a). Reference $y_2(t)$ is used to describe the headphone-to-eardrum transfer function:

$$Y_2(f) = E(f) \cdot C(f) \cdot M(f) \cdot X_0(f) \qquad \text{(Eq. 3.6)}$$

with E(f) denoting the earphone and C(f) the ear canal transfer function. The appropriate filter $V_{\phi\theta}(f)$ is then calculated by dividing the transfer function Y_0 and Y_2:

$$V_{\phi\theta}(f) = \frac{Y_0(f)}{Y_2(f)} = \frac{L(f) \cdot H_{\phi\theta}(f)}{E(f)} \qquad \text{(Eq. 3.7)}$$

The thus obtained transfer function for the right and left ear $V_{\phi\theta}(f)$ describe the appropriate filters to simulate any sound signal from the direction ($\phi\theta$). Note that the transfer function of the ear canal is cancelled out. It was not compensated for the loudspeaker's transfer function since it was flat within ±3 dB in the important frequency range from 2-12 kHz. It is important to note that the transfer function of the earphones E(f) is cancelled out as well (Eq. 3.8). When the earphones are used for stimulation their transfer function appears in the denominator and in the nominator and can thus be cutted from the equation.

$$V_{\phi\theta}(f) \cdot E(f) = \frac{L(f) \cdot H_{\phi\theta}(f)}{E(f)} \cdot E(f) = L(f) \cdot H_{\phi\theta}(f) \qquad \text{(Eq. 3.8)}$$

2.3 Results

2.3.1 HRIRs and spatial patterns of broadband ITD and ILD

The typical time course of HRIRs is shown in Fig. 2.1 for owl J. As described by Poganiatz (2000), for most positions in space a characteristic feature of the HRIRs is a large positive peak followed by a smaller negative trough. The shape of the functions for both ears at one position in space showed some minor differences that are attributable to the asymmetry of the ears. Frontal positions showed larger amplitudes than such in more peripheral locations. Moreover, the amplitude decreased with deviations from 0° in the elevational plane. The highest amplitude was found in front of the owl (ϕ: 0° and θ: 0°). This indicates a strong directionality of the owl's facial ruff.

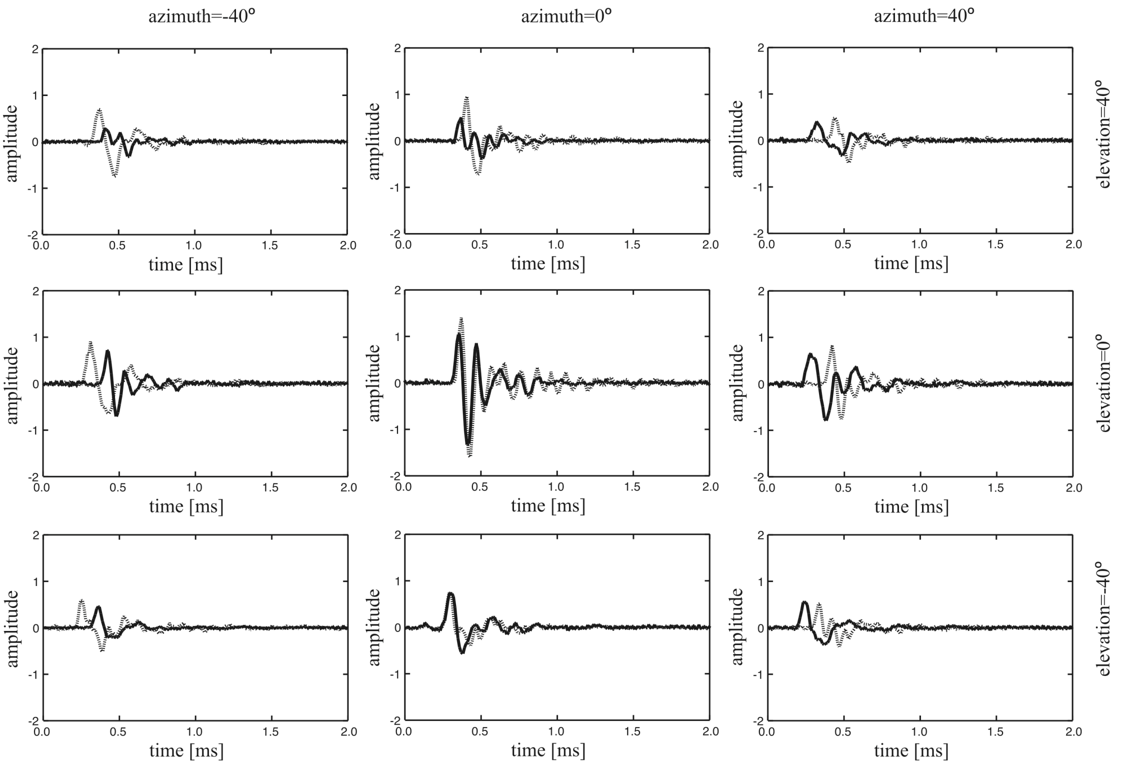

Fig. 2.1 HRIRs of both ears for 9 positions in space from owl J. Subplots in one column show data obtained at same azimuth while subplots in one row show data from the same elevation. The black line represents the HRIR of the right, the grey line of the left ear. For negative values of azimuth the sound arrives at the left ear first. The right ear leads at positive values. The amplitude of the HRIRs depends on elevation. Note that the HRIRs for ϕ: 0° and θ: 0° show the highest amplitude and little differences in the shape of the functions which are attributable to the asymmetry of the owl's ears.

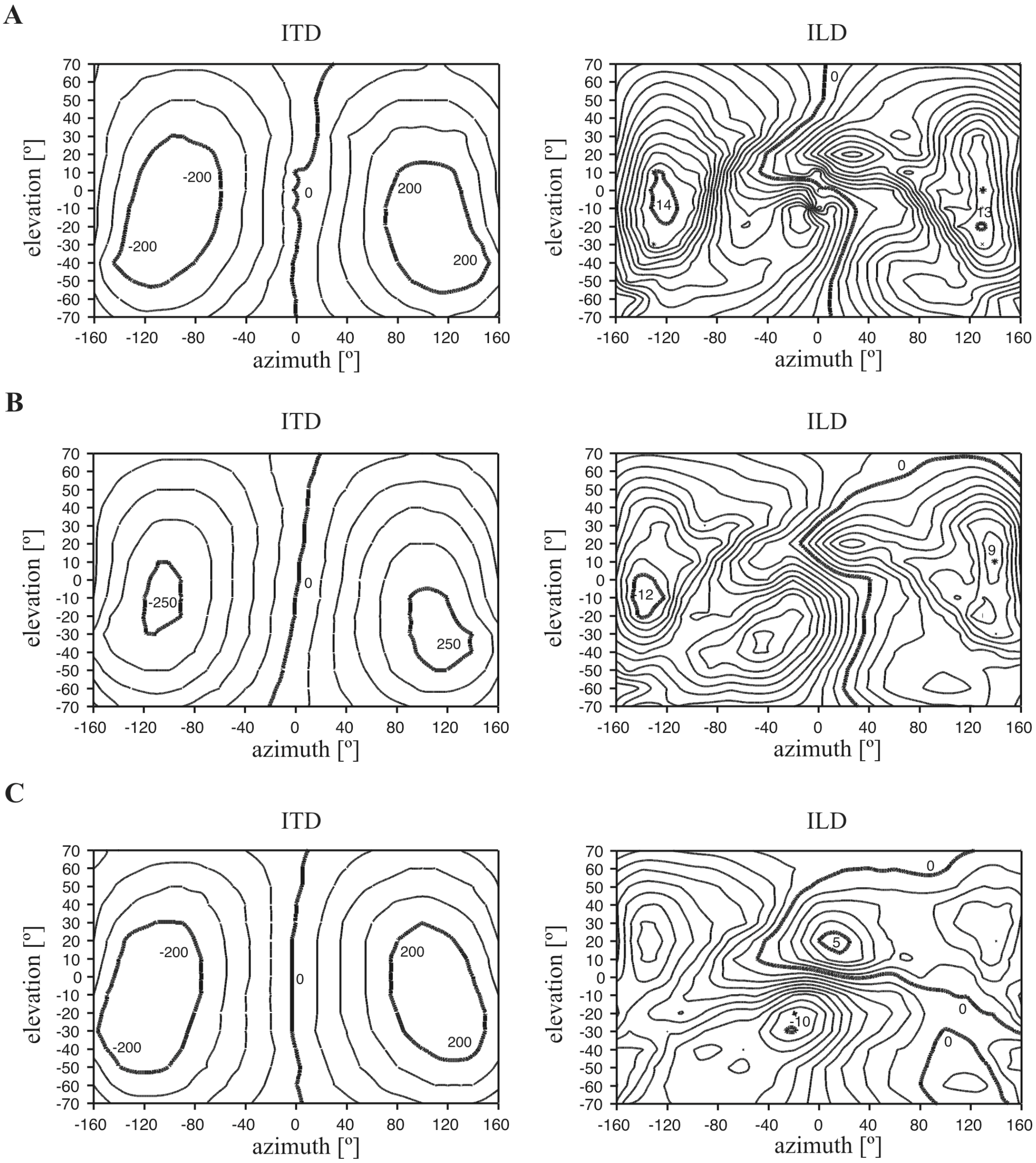

Fig. 2.2 Spatial patterns of broadband ITD and ILD for the three owls. The iso-ITD contour lines are drawn at intervals of 50 μs, with the right ear leading at positive values. Iso-ILD contour lines are drawn at intervals of 1 dB, with positive values indicating that the signal is louder in the right ear. Spatial positions are given in spherical coordinates. 0° azimuth and 0° elevation represents the front of the owl. Positive angles denote the right or upper hemisphere, respectively. The thick lines mark the maximum, zero and minimum contour lines in each plot. **A** ITD and ILD pattern for Owl O. **B** Same as in **A** for Owl S. **C** Same as in **A** for Owl J.

To calculate the ITD from a pair of HRIRs a cross-correlation was performed. The accuracy of this calculation is limited by the sampling rate at which the signal was recorded. The used sampling rate of 100 kHz led to an accuracy of ±10 μs. For all three owls the ITD between the first peak of the HRIR of the right and left ear increased to the periphery with a centre of symmetry at about 100° and –100° azimuth, respectively (Fig. 2.2 left column). The ITD varied mainly with azimuth (for a statistical analysis see Poganiatz 2000). At ϕ: 0° and θ: 0° the ITD is 0 µs, at ϕ: 40° and θ: 0° about 100 µs. The right ear leads at positive angles and vice versa. The largest ITD found was 260 µs for owl S.

The calculation of ILD was done by subtracting the mean energy of the HRTFs in the frequency range from 2-12 kHz in dB of the right and left ear. The partial pattern obtained was more complicated than the ITD pattern (Fig. 2.2 right column). No symmetry could be found. ILDs varied between –14 and 13 dB for owl O, between –12 and 9 dB for owl S and between –10 to 5 dB for owl J. The difference between both ears was accordingly between 15 and 27 dB in all three owls. Between ±30° azimuth and ±30° elevation the ILD changed systematically in the vertical direction. 0 dB ILD of owl J in contrast to that of the other two owls was shifted rightwards. This changed the position of maximum and minimum ILD to ±30° azimuth and ±30° elevation. The extrema were located in more peripheral azimuthal and more central elevational locations in the two other owls.

2.4 Discussion

The results obtained are consistent with those of previous studies (Keller et al. 1998; Poganiatz 2000). For all three owls broadband ITD changed with azimuth. The time-scale of ITD ranged from around –250 to 250 µs, with 0 µs being at 0° azimuth. The centre of symmetry for ITD found at ±100° is equal to the owl's anatomical symmetry centre.

In contrast to this, no such centre of symmetry was found for ILD. This is attributable to the asymmetrical position of the owl's ears. In the frontal field ILD changed from the lower left to the upper right. The distribution of maximum and minimum was symmetrical in two owls. Both extrema were found at peripheral azimuth positions around 0° elevation. In owl J the maximum lay in the upper half of the lower right hemisphere and the minimum in the lower left hemisphere. Moreover, the overall ILD pattern was not identical between the individual owls. Little differences became apparent, the most important being the rightward shifted pattern of owl J. As described by Poganiatz (2000) characteristic and individually different notches appear in the monaural spectra at high frequencies in the rear positions causing the noticed differences in the ILD patterns. In addition, the anaesthesia leads to a slightly unnatural position of the owl's facial ruff and ear flaps, and since the ILD is strongly influenced by these anatomical features (Coles and Guppy 1988; Payne 1971). The change in the ILD pattern could thus be explained. This seems to be the main reason for owl J's shifted pattern of ILDs.

As an important issue, it should be kept in mind that the amplitude of the HRIRs declined towards the periphery. That is, sounds from lateral positions are fainter compared to sounds coming from the front (directionality of facial ruff). This is important for the electrophysiological experiments described in this thesis as will be seen in chapter 3.

2.4.1 Methodological aspects

To assess possible problems occurring in the electrophysiological experiments, it is necessary to analyse potential systematic errors introduced by the HRTF measurement.

The main difficulty measuring HRTFs of owls is the placement of the microphones and earphones (reference measurement 2). In this study no attempt to implant metal holders that allow an invariant positioning of microphones or miniature earphones (Keller 1998) to the ear entrance was made. Instead, the insertion depth of the microphones was controlled via a scale on the microphone tubes (Poganiatz 2000). In this approach the vertical and horizontal position could not be monitored. However, with the assumption that the ear canal can be approximated as a tube, the sound pressure will be constant for wavelengths smaller than the diameter of the ear canal. In the case of the barn owl, sound pressure differences can be neglected for frequencies up to 10 kHz (Poganiatz 2000) since the diameter of the ear canal is less than 8 mm. In addition, the spiral form of the ear canal restricted the placement of the microphone.

Another potential error source is the placement of the earphones during the measurement and as well during the experiment. Since from-the-shelf Sony earphones were used, some problems arose. First, the speaker's membrane was eccentric, so special care must be taken to place the phones correctly. This leads to the second problem. Due to the size of the earphones, the owl's ear flaps restricted the placement of the phones. For each owl reference measurement 2 was repeated three times or more to assess the influence of earphone position. An offline comparison using different reference measurements for ITD and ILD calculation showed no obvious deviations between the slightly different earphone positions.

2.5 References

Coles RB and Guppy A (1988) Directional hearing in the barn owl (*Tyto alba*). *J. Comp. Physiol A* 163: 117-133.

Keller CH, Hartung K, Takahashi TT (1998) Head-related transfer functions of the barn owl: measurement and neural responses. *Hear. Res.* 118: 13-34

Payne RS (1971) Acoustic location of prey by barn owls (*Tyto alba*). *J. Exp. Biol.* 54: 535-573

Poganiatz I (2000) Sound-localization in barn owls – Experiments with virtual space stimuli – *PhD-Thesis at the Reihnisch-Westfälische Technische Hochschule Aachen*

Wagner H (1993) Sound-localization deficits induced by lesions in the barn owl's space map. *J. Neuroscience* 13: 371-386

Wightman FL and Kistler DJ (1989a) Headphone simulation of free-field listening I. Stimulus synthesis. *J. Acoust. Soc. Am.* 85: 858-867

Wightman FL and Kistler DJ (1989b) Headphone simulation of free-field listening I. Psychophysical validation. *J. Acoust. Soc. Am.* 85: 868-878

Yost WA and Dye RH (1997) Fundamentals of directional hearing. *Seminars in hearing* Volume 18, Number 4: 321-344

Chapter 3

Electrophysiological experiments with FixT and AddT stimuli

Behavioural studies with free-field, non-virtual and virtual dichotic stimuli have shown that interaural time difference (ITD) is the main cue for the barn owl's judgement of azimuth. However, direct electrophysiological evidence supporting this finding is still missing. So far electrophysiological studies focus on space-specific midbrain neurons in the owl, suggesting that ITD is not the only cue to influence the tuning properties of neurons in the external nucleus of the inferior colliculus (ICx) and the optic tectum (OT). Therefore, in this thesis the virtual acoustic space (VAS) technique was employed to investigate the tuning properties of neurons from lower stages of the auditory pathway, known to respond to single spatial cues. Manipulation of the virtual stimuli by fixing the ITD to a constant value for frontal spatial positions while leaving all other spatial cues unchanged led to a loss of tuning for 71% of the units recorded in the core of the central nucleus of the inferior colliculus (ICc-core) while the majority of units of the lateral shell of the central nucleus of the inferior colliculus (ICc-ls) changed their tuning properties unpredictable. Introducing an additional time delay to the virtual stimuli led to a predictable shift of the neuron's azimuth tuning. Thus, ITD is the only cue necessary to code azimuth in ICc-core.

3.1 Introduction

Is ITD the only parameter necessary for coding azimuth in the barn owl's midbrain? To address this question, neurons from ICc-core were recorded using virtual acoustic stimuli (VAS) replicating the naturally occurring free-field situation and manipulated virtual stimuli to test whether a systematical manipulation of ITD for each simulated position in space leads to predictable changes in the azimuthal tuning of these neurons.

3.1.1 The auditory pathway of the owl

Since in the sensory organ for sound perception – the cochlea – the frequencies of a sound source and not its position in space are represented, the spatial information essential for sound localization needs to be extracted from the features inherent to the sound. The two naturally occurring binaural cues are the interaural time difference (ITD) and interaural level difference (ILD) as described in the previous chapters. In the owl these are represented in two anatomically different pathways up to the level of the midbrain (Fig. 3.1). In the external nucleus of IC (ICx; Takahashi and Konishi 1986; Wagner et al. 1987; Mazer 1998) and the optic tectum (OT; Knudsen 1982), space-specific neurons are organized in a map of acoustic space. Hence, at this stage of processing all relevant information about the location of a sound is combined and coded by the responses of ICx and OT neurons. But how is this computation achieved? In the following a description of the main computational steps in the time pathway is given (for a more detailed review see Konishi 2003).

In his seminal paper on the place theory of sound localization Jeffress (1948) proposed a model in which an array of neurons that receives ordered input from systematically delayed ipsi- and contralateral projections fires maximally when the input from both sides arrive at the same time, e.g. acoustic and neuronal delay from both sides are equal (coincidence detector). This model was the first approach to theoretically describe the prerequisites a neuronal system must fulfil to extract information about ITD. Such an array was later found in the avian nucleus magnocellularis (NM) and the nucleus laminaris (NL; chicken: Parks & Rubel 1975; owl: Sullivan & Konishi 1984). Axon collaterals of the NM form the systematically delayed input integrated by the somata of neurons in the NL. The computation of ITD is frequency-dependent and similar to a cross-correlation.

Neurons from the NL project to the contralateral core of the central nucleus of the inferior colliculus (ICc-core). These neurons are narrowly tuned to frequency, binaurally balanced and are sensitive to ITD only (Tab. 3.1). Their response varies in a cyclic manner with maxima at integer multiples of the period of the stimulating frequency or best frequency if stimulated with noise (Wagner et al. 1987; Wagner et

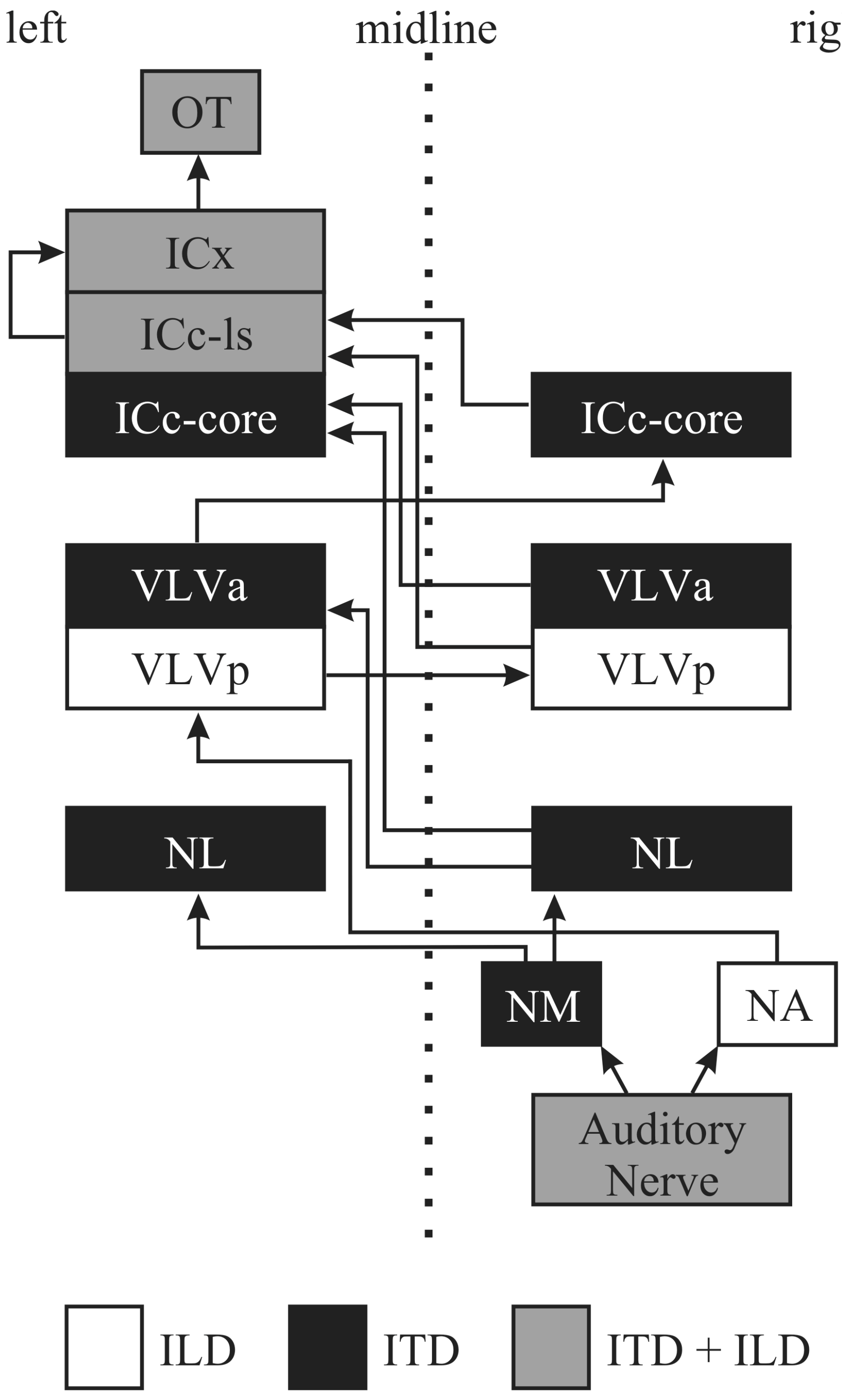

Fig. 3.1 Binaural processing in the barn owl's brainstem. White: Nuclei involved in ILD processing Black: Nuclei involved in ITD processing. Grey: Nuclei involved in processing both cues. At the stage of the ICx both cues are used to compute a space map. ICx neurons are space-specific. Abbreviations: *ICc-core* – core of the central nucleus of the inferior colliculus; *ICc-ls* – lateral shell of ICc; *ICx* – external nucleus of the inferior colliculus; *NA* – Nucleus angularis; *NL* – Nucleus laminaris; *NM* – Nucleus magnocellularis; *VLVa* – Nucleus ventralis lemnisci laterale pars anterior; *VLVp* – Nucleus ventralis lemnisci laterale pars posterior. Modified from Poganiatz 2000.

Tab. 3.1 Important characteristics of the single IC subdivisions, due to which a physiological classification is possible. Abbreviations: *d* – dorsal; *EE* – Contra- and ipsilateral excitatory; *EI* – Contra excitatory, ipsi inhibitory, *f* – frequency, *pa* – Phase ambiguous. From: Wagner (Personal communications)

Nucleus	Frequency	ITD	ILD	Contra/Ipsi	Latency
ICc-core	d→v: low → high 300 Hz → 11 kHz narrow f-tuning	tuned pa ipsi array	not tuned	EE	5-7 ms
ICc-ls	similar to core, sharp f-tuning	tuned pa contra array	tuned with broad maximum	EI	6.5-8 ms
ICx	broad f-tuning no clear tonotopy noise better than tone	tuned no pa	tuned	exclusively binaural	8-12 ms

al. 2002). Hence, ICc-core neurons signal phase differences between both ears in an ambiguous manner since these differences correspond to more than one ITD (phase ambiguity). Nevertheless, one specific ITD elicits the same response rate in all neurons of an anatomical and physiological unit, or array. This ITD is called the array-specific ITD. The arrangement in these arrays with, in addition, frequency represented from low to high in a dorsal to ventral manner leads to a systematic map of the entire physiological ITD-range in ICc-core (Wagner et al. 1987; Wagner et al 2002). However, only ipsi-lateral space is represented (ipsi array).

ICc-core neurons project to the lateral shell of the ICc (ICc-ls; Takahashi et al. 1989). ICc-ls neurons are similar to ICc-core neurons in their ITD sensitivity and tonotopic organization but are ILD sensitive in addition (Tab. 3.1; Adolphs 1993; Mazer 1998). This derives from additional input from the nucleus angularis (NA) via the nucleus ventralis lemnisci laterale pars posterior (VLVp).

Receiving its input from the ICc-ls, the external nucleus of the IC (ICx) is the first station with a physiological space map computed from the interaural differences. Neurons from the ICx only respond to stimuli from a particular position in space (Knudsen and Konishi 1977, 1978; Wagner et al. 1987). Since these space-specific neurons integrate the input from a wide range of frequency-specific neurons from an ITD array of the ICc-ls, they exhibit a broad frequency tuning and show no phase ambiguity if stimulated with noise (Takahashi and Konishi 1986; Peña and Konishi 2000). Their systematic arrangement in a map of acoustic space is projected to the last midbrain nucleus, the OT (Knudsen and Knudsen 1983). The OT is a multimodal structure combining sensory information from different modalities with motor action (Masino and Knudsen 1990; du Lac and Knudsen 1990).

Summing up, in earlier stages neural populations code spatial parameters in narrow frequency bands, for example in ICc-core where interaural phase differences are coded. Positions of space are represented in ICx for the first time in the ascending auditory pathway. This space map is then projected to OT where sensory-motor integration takes place. Therefore, if one wants to study the influence of one of the binaural spatial cues on coding of space, earlier stages of the auditory pathway should be considered. Since in higher regions due to the computation of space maps different cues are intermingled and therefore not easily controlled or separated.

3.1.2 FixT and AddT stimuli

As said above, if ITD is the only parameter influencing the tuning properties of ICc-core neurons, a systematical manipulation of ITD should lead to predictable changes in azimuthal tuning. First of all it is necessary to understand the naturally occurring situation before one tries to comprehend the manipulated virtual stimuli.

When a sound reaches the ears from azimuth ϕ 0° and elevation θ 0°, ITD is zero (Fig. 3.2 A middle). In contrast, a sound emitted from a source at ϕ 40° and θ 0° reaches the left ear 100 µs after the right ear (Fig. 3.2 A right). Exactly the opposite is the case for sounds emitted from the left site at ϕ –40° and θ 0° (Fig. 3.2 A left). Then the sound at the right ear lags 100 µs. Moreover, it is important to bear in mind that sounds reaching the ears from peripheral positions are attenuated due to the high directionality of the owl’s facial ruff.

All these characteristics of sounds emitted from different positions in space can be simulated by head related impulse responses (HRIR) that can be used as digital filters to create virtual acoustic space stimuli (see chapter 2). The HRIRs allow a manipulation of one of the different binaural cues without altering any of the others.

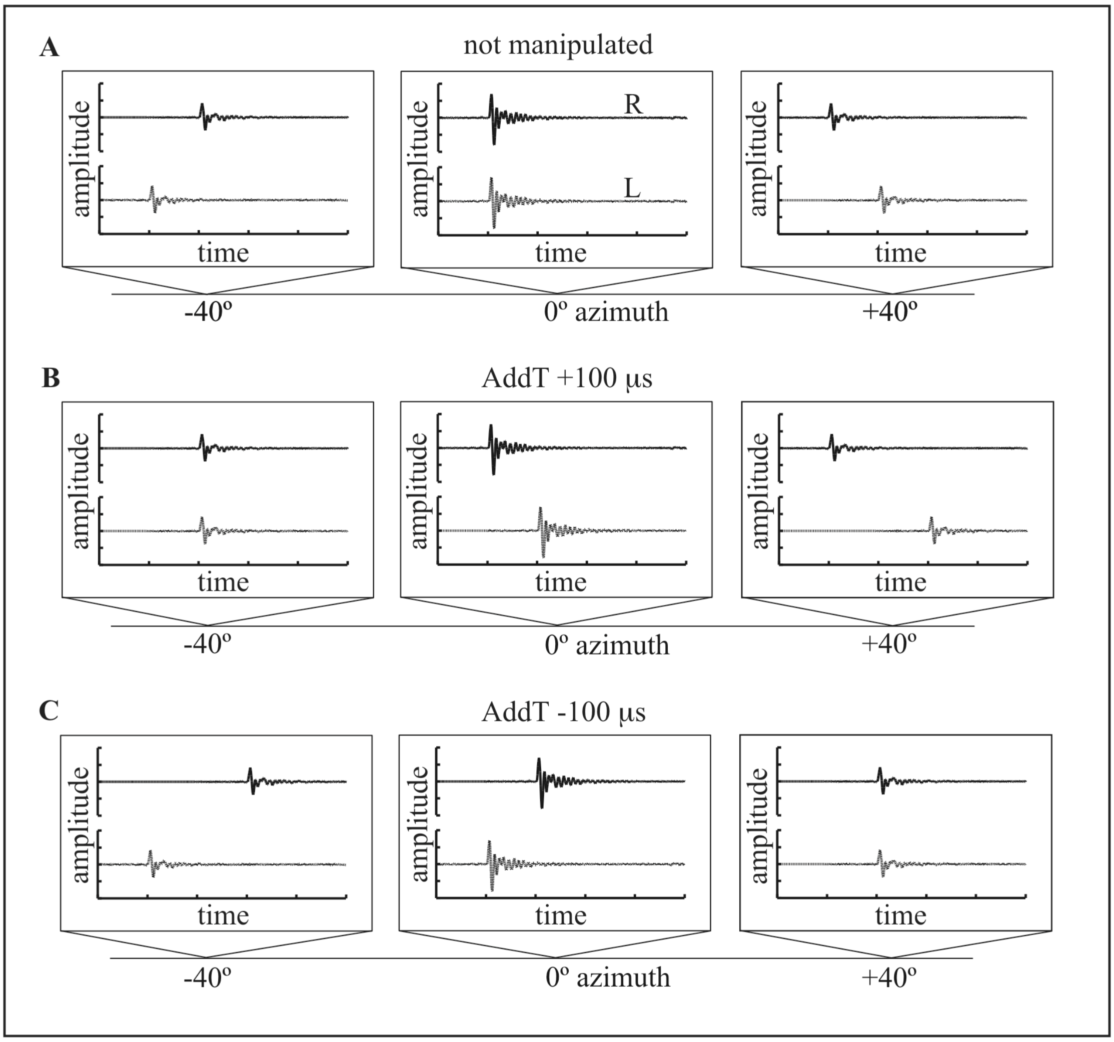

Fig 3.2 HRIRs as a function of amplitude over time for natural and manipulated virtual stimuli at azimuth ϕ -40°, 0° and 40° all at elevation θ 0°. Upper black trace: HRIR of the right ear; lower grey trace: HRIR of the left ear. The sound reaches the right ear first at positive values of ϕ; at negative ones it reaches the left ear first. Note that the HRIRs (duration 1 ms) and the time shift (100 µs) are not drawn to scale. All plots are drawn relative to each other for a better comparability. **A** Natural situation. No ITD at ϕ 0; at ϕ 40° the right ear leads by 100 µs; at ϕ -40° the left ear leads by 100 µs. **B** AddT +100 µs. See text for details. **C** AddT -100 ms. See text for details.

One possibility to manipulate virtual stimuli is to introduce an additional time delay adding up to the naturally occurring one (Fig. 3.2 B). The addition of a 100 µs delay to the HRIR of the left ear representing ϕ 0° and θ 0° resembles the natural ITD situation at ϕ 40° and θ 0°. In contrast, ILD and monaural cues still point towards ϕ 0° and θ 0°. These stimuli are called $AddT_x$ stimuli (Poganiatz 2000), with x denoting the added delay in µs. Positive values indicate that the additional delay was introduced to the HRIR of the left ear (Fig. 3.2 B), negative values that it was introduced to the HRIR of the right ear (Fig. 3.2 C). A neuron in ICc-core should respond to AddT stimuli in the following way. Independent of the spatial position coded by the unmodified HRIRs the neuron should respond to positions whose combined natural and added delay correspond to the neuron's characteristic ITD. Imagine a neuron responding best to an ITD of 100 μs, corresponding to ϕ 40° (Fig. 3.2 A right). The introduction of an additional delay of +100 μs to the HRIRs shifts the maximum response of that specific neuron from ϕ 40° to ϕ 0° (Fig. 3.2 B middle). Due to the manipulation the only position in space that has a combined natural (0 μs) and added delay (100 μs) of 100 μs is ϕ 0°. Thus, when recording a rate-azimuth function (RAF), e.g. recording the response of a neuron to different azimuth positions with a constant setting for elevation, the response maximum of that neuron will shift in a predictable way if ITD is the only parameter influencing its tuning properties.

The second manipulation employed in this thesis is the fixation of HRIRs to one ITD over the whole azimuthal range. These stimuli are called FixT stimuli (Poganiatz et al. 2001). By fixing the ITD to the neuron's best ITD its characteristic tuning maximum should be lost. Instead the neuron should respond to all tested azimuthal positions with the same maximal firing rate, if only ITD is important for tuning in azimuth. Nevertheless, one issue remains. Since the overall level of the stimuli decreases towards the periphery, the firing rate decreases also (Poganiatz 2000). This leads to unpredictable changes in the neuronal response for stimuli presented in the periphery. Thus, it is necessary to adjust for these differences in overall level. In this study the average binaural level (ABL) was calculated to compensate for the effect described.

3.2 Methods

Experiments were carried out with three barn owls from the Institute's breeding colony that will be referred to as owl J, O and S. Each owl was used for several electrophysiological experiments in intervals of two weeks. All experiments were carried out in accordance with German Law and the NIH guidelines for care and use of laboratory animals and were approved by the Regierungspräsidium Köln.

3.2.1 Surgery and electrophysiological procedures

All experiments including either surgery or electrophysiology were performed under anaesthesia (Ketamin 20 mg/ kg body weight/h; Sanofi-CEVA GmbH, Düsseldorf). In addition, the animals were tranquilized with Diazepam (Valium 1 mg/kg/h; Merckle GmbH, Blaubeuren). To prevent salivation Atropine sulphate (0.05 mg/kg; Braun Melsungen AG, Melsungen) was injected at the beginning of the experiment. The fixation of the owl in the sound-attenuating chamber was carried out as described in chapter 2. Thereafter, a craniotomy was conducted to expose a part of the dural surface. In all owls this was done on the left hemisphere. An insulated tungsten microelectrode (Frederick Haer Co., 13-15 MΩ) was positioned with respect to the metal post of the stereotaxic device that served as a reference. The electrode was advanced through the brain from dorsal to ventral via a remote-controlled stepping motor. Extracellular recordings of action potentials of neurons were amplified with an amplifier (M. Walsh Electronics), digitized with an AD converter (Tucker Davis Technologies, Gainesville) and passed to a computer (x86 family) for storage and an audio-monitor for acoustical online control. Stimulation and recordings were synchronized with Jan Schnupp's Brainware for TDT's System II (Version 6.1.1).

The experiments lasted between 12 and 17 hours. At the end of the experiment the craniotomy was closed with dental cement. A topical antibiotic (Nebacetin; Ymanouchi Pharma GmbH, Heidelberg) ointment was applied before closing the skin incision. Subsequently, the owl was put into a wooden box for recovery. Owls did not exhibit any signs of uneasiness and ate normally the day after the experiment.

3.2.2 Stimulus Generation

Two kinds of stimuli presented via earphones were used during the electrophysiological experiments. Simple dichotic stimuli that consisted either of fresh white noise or pure tones with an interaural time delay, an interaural level difference or with varying attenuation were used. Stimuli were generated with TDT's system II (DA1, PA4, FT6 Tucker Davis Technologies, Gainesville; Yamaha AX-590 amplifier) using Jan Schnupp's Brainware (Version 6.1.1) for interfacing with custom written dlls. All stimuli were ramped (5 ms rise/fall time, $\sin^2$) and had a duration of

100 ms. These stimuli were used for orientation during the advancement of the electrode and characterization of the units during an experiment.

Virtual stimuli were created, convolving the stored HRIRs (see chapter 2) with 100 ms fresh white noise via the TDT system. In addition to these, manipulated virtual stimuli were generated with procedures written in MatLab (The Mathworks, Version 6.5.1) to test the influence of ITD on the spatial tuning properties of neurons while all other cues remained unchanged. ITDs were manipulated in two different ways. They were either fixed at a constant value for both ears or shifted by introducing an additional time delay to one of the ears.

ITDs were fixed by shifting the HRIRs of the right and left ear to the maximum of their cross-correlation function. This leads to an artificial zero ITD situation for all sampled spatial positions while on the same time ILD and monaural cues remain unchanged. This manipulation leads to small frequency-dependent changes of the phase spectrum. To avoid distortions of the HRIR shape no attempt to correct these changes were made. The thus obtained fixed HRIRs were stored on disk. During an experiment an additional time delay was introduced via the sound generating system to fix the ITD of the stimuli to the unit's best ITD.

In addition the average binaural level (ABL) was calculated as the sum of the root mean squared amplitudes of the HRTFs of the left and right ear divided by two (Peña et al. 1996; Miller and Knudsen 1999; Euston and Takahashi 2002). This was done for all sampled spatial positions for the frequency range from 2 to 12 kHz (hereafter referred to as broadband noise or noise) and for a number of 1/6-octave bands centred on several specific frequencies (hereafter denoted by the corresponding centre frequency). This resulted in a set of values for the broadband noise and for each of the 1/6-octave frequency bands. The ABL-values obtained were used to scale the filtered stimuli so that the average of the right and left root mean squared amplitude was identical for all spatial locations (note that this did not alter ILD or monaural cues). The usage of the ABL-correction could be chosen via Brainware. These stimuli are denoted as $\mathrm{FixT}_{\mathrm{x}\ \pm\mathrm{abl}\ 1/6\text{-octave frequency band}}$, with "x" being the fixed ITD in μs, "abl" indicating that the ABL-correction is either used (+) or not (-) and "1/6-octave frequency band" indicating the centre frequency of the 1/6-octave band used or if denoted as "noise" this indicates the use of broadband noise.

Introducing an additional time delay to their natural ITD either to the right or left channel with the sound generating system generated the second type of manipulated virtual stimuli. These stimuli are referred to as AddT_x, with x denoting the additional ITD shift in microseconds.

3.2.3 Data collection

Electrophysiological recordings were made from the core of the central nucleus of the inferior colliculus (ICc-core) and the lateral shell of the central nucleus of the inferior colliculus (ICc-ls) on the left side of each owl. The optic tectum (OT) and the different subdivisions of the IC were identified by characteristic tuning properties of the units that are known from literature (Knudsen and Konishi 1978; Moiseff and Konishi 1983; Knudsen 1984; Takahashi and Konishi 1986; Wagner et al. 1987; Takahashi et al. 1989; Fujita and Konishi 1991; Adolphs 1993). While advancing the electrode search stimuli were presented consisting of broadband white noise with systematically changing ITD and ILD. The recording was started, if an acoustically driven unit could be isolated from the neuronal background. Recording started 100 ms before stimulation (pre-stimulus onset) and stopped 400 ms after the stimulus ended (post-stimulus time) with an inter-stimulus time of 1 s. The presented sequence of sounds consisted of 19 (ITD and frequency), 11 (ILD), 12 (attenuation) different stimuli each repeated 5 times in a pseudo-random order.

First, the ITD tuning of the unit was recorded. Second, the ILD tuning was measured at the ITD value, at which the unit responded best. If not otherwise stated ITD and ILD tuning curves were recorded using broadband white noise for stimulation. Third, a frequency tuning was recorded with pure tones ranging from either 200 to 3800 Hz (Δ200 Hz) or 200 to 9200 Hz (Δ500 Hz). Fourth, monaural rate-level functions (RLFs) for both ears were recorded. Fifth, a rate-azimuth function (RAF) was recorded for ICc-core and ICc-ls units ranging from –160° to 160°. In addition, rate-elevation functions were measured for ICc-ls and for several ICc-core units. Finally, several or all manipulated stimuli were tested either with or without ABL-correction depending on the stability of the extracellular recording. Broadband noise was used to record ITD-, ILD functions, RLFs, RAFs and manipulated RAFs, if not otherwise stated. All other parameters were adjusted to the unit's best values.

Stimulus level was set 20 dB above threshold, which was determined via the RLFs. A typical recording done this way lasted for about an hour.

3.2.4 Data analysis

Single units (SU) were isolated from multi units (MU) if possible by online and offline cluster cutting with the recording software (Jan Schnupp's Brainware, Version 6.1.1). Further offline analysis was carried out with MatLab (The Mathworks, Version 6.5.1). To obtain the tuning curves, spike numbers for the five repetitions of a stimulus were averaged and corrected for the spontaneous activity that was determined from the spike rate measured before stimulus onset. This resulted in a negative spike rate for inhibited units. In addition, the corrected spike numbers of each single stimulus presentation were used for statistical analysis for tuning (Kruskal-Wallis test, $p<0.05$). Units were classified as "tuned" if the average spike rate of at least one of the presented stimuli differed significantly from the other spike rates, otherwise units were classified as "not tuned". Visualization was done with IGOR Pro (Wavemetrics, Version 5.03).

3.3 Results

3.3.1 General observations

The database consists of a total of 48 units in 13 experiments from three animals. 31 units were recorded in ICc-core, 17 in ICc-ls. A unit was classified as single unit (SU) if its action potential shape could clearly be distinguished from the background via cluster sorting (Brainware Version 6.1.1). This means that units were classified as multi unit (MU) if it was not possible to avoid the potential inclusion of background activity or the false rejection of the unit's activity. Therefore, only one ICc-core and one ICc-ls unit were classified as single unit. Nevertheless, due to the tonotopic or topographic arrangements of neurons in maps in the investigated brain areas no significant differences between the results from multi and single units were expected (Wagner et al. 1987).

Fig. 3.3 shows an ITD tuning function, the corresponding raster-plot, together with action potential shapes of the unit and the background. The unit was classified as MU. Note the high background activity before the stimulus and its temporary decrease after stimulus presentation in the raster plot. The high spontaneous spikerate

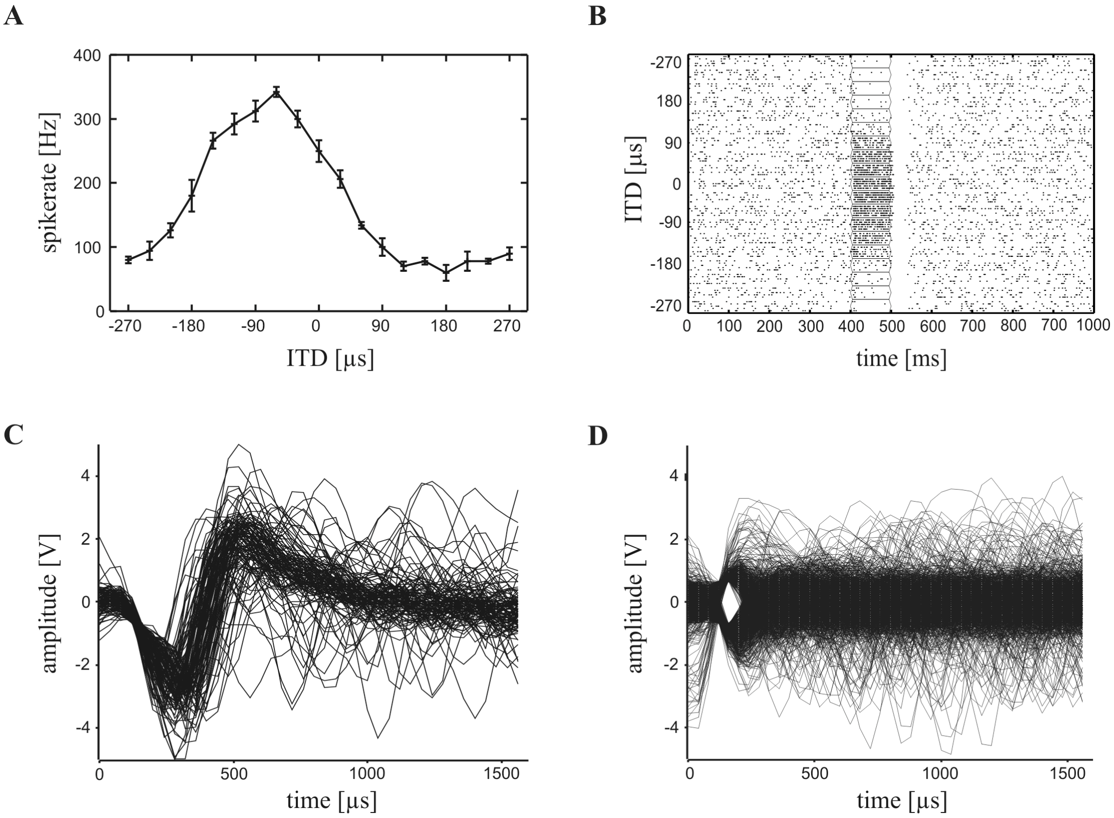

Fig. 3.3 **A** ITD tuning function of a typical ICc-core unit. The function was obtained by adjusting ILD to the unit's best value while stimulating with noise. Error bars indicate the standard deviation. **B** Corresponding raster-plot **C** Shape of the action potential for the unit shown in **A** and **B**. This unit was classified as MU. **D** Corresponding shape of the background.

was characteristic of more dorsal ICc-core neurons. More ventrally located neurons exhibited less background activity.

Since the measurement program lasted for nearly one hour the recording conditions sometimes changed or the unit was lost, so that it was not possible to collect a complete set of tuning functions for all units. Three units from ICc-core and five units from ICc-ls could thus not be used for analysis.

3.3.2 Responses of ICc-core units to dichotic and natural virtual stimuli

The characteristic tuning properties of ICc-core units as they are known from literature (Wagner et al. 1987; see also Tab. 3.1) helped to identify the target area. Units were classified as ICc-core when tuned to ITD and azimuth according to the Kruskal-Wallis test ($p<0.05$) and were not tuned to ILD (Kruskal-Wallis test; $p>0.05$). In addition they showed phase ambiguity and were sharply tuned to frequency (Fig.

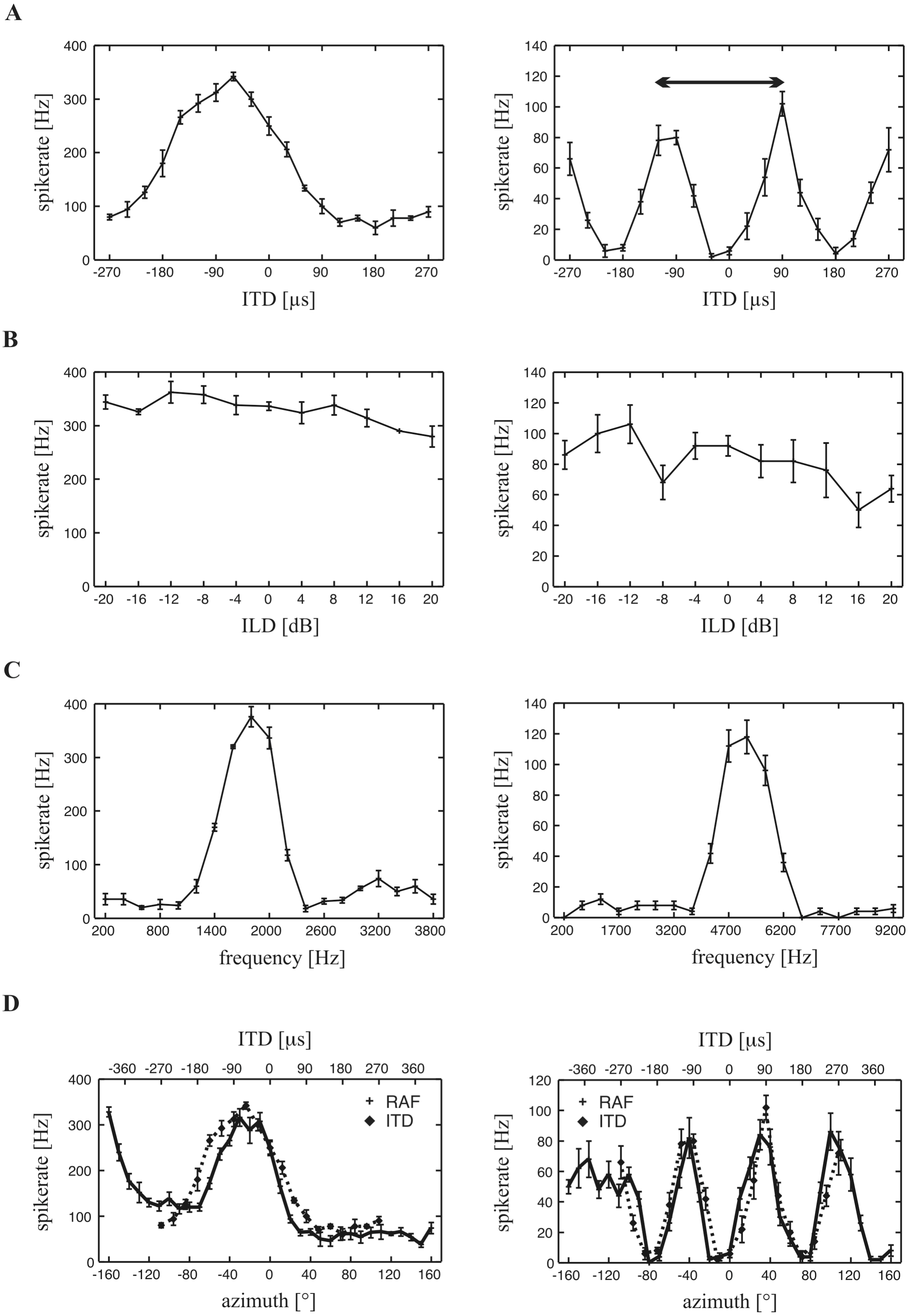

Fig. 3.4 Tuning curves for a representative low-frequency (left column) and high-frequency (right column) ICc-core unit to ITD, ILD, frequency and azimuth. Functions for one parameter were obtained by adjusting all other parameters to the unit’s best values. Error bars indicate the standard deviation. The highest mean spontaneous activity for the low-frequency unit was 1.3±0.8 Hz and for the high-frequency unit 39.2±5.3 Hz. **A** ITD tuning curve **B** ILD tuning curve **C** Frequency tuning curve **D** RAF (crosses) and ITD (diamonds) tuning curves. Note the different abscissas for ITD and azimuth.

3.4 A-C). The frequency to which the units responded best changed systematically from low to high during a dorsal to ventral advancement of the electrode. The tuning to ITD showed a periodicity equivalent to the inverse of the unit's best frequency as can be seen for the unit presented in the right column of Fig. 3.4. The period of the ITD tuning curve (Fig. 3.4 A) was 210 µs as indicated by the arrow. The frequency of 4762 Hz accordingly calculated corresponds well to the unit's best frequency of 5200 Hz.

As can be seen from Fig. 3.4 D the units' RAF was comparable to their ITD-function. In accordance with literature (Poganiatz 2000), a relationship between azimuthal and ITD tuning was found (Fig. 3.5). A simple linear regression between the ITD and azimuthal tuning maximum closest to 0 µs or 0°, respectively, yielded the following equation:

$$\text{azimuth [°]} = 3.7656 \pm 7.31° + 0.38875 \pm 0.0573°/\mu s * \text{ITD } [\mu s] \qquad \text{(Eq. 3.1)}$$

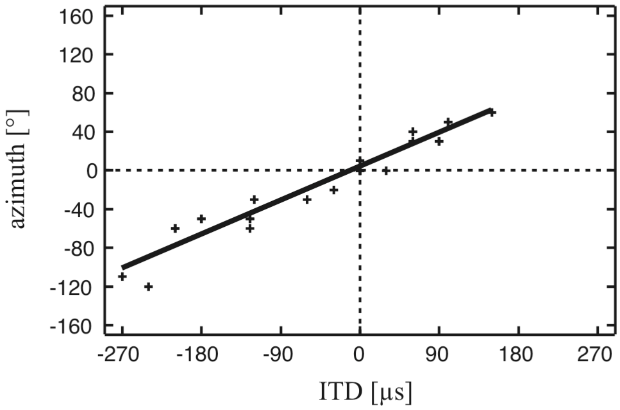

Fig. 3.5 Best azimuth plotted versus best ITD. 14 of the 31 ICc-core units showed identical azimuth and ITD combinations. The parameters were positively correlated (N=31, $p<0.01$, $R^2=0.968294$).

3.3.3 Responses of ICc-core units to FixT stimuli

The influence of ITD on azimuthal tuning of ICc-core units was investigated via manipulated virtual stimuli with fixed ITD values. In these stimuli all spatial parameters were unchanged except for the ITD, which was fixed to the unit's best ITD value as obtained by dichotic stimulation. Thus, all parameters except for the ITD pointed towards the position in space that was originally encoded by the HRTFs. Four subtypes of FixT-stimuli were tested:

(1) $\text{FixT}_{\text{x -abl noise}}$

(2) $\text{FixT}_{\text{x -abl 1/6-octave frequency band}}$

(3) $\text{FixT}_{\text{x +abl noise}}$

(4) $\text{FixT}_{\text{x +abl 1/6-octave frequency band}}$

"x" denotes the unit's best ITD in μs, "abl" indicates that the ABL-correction is either used (+) or not (-), "noise" that the unit was stimulated with broadband noise and "1/6-octave frequency band" that it was stimulated with an 1/6-octave frequency band centred at the unit's best frequency.

These manipulations led to an observable change of the RAFs for all units tested. Usually, units responded at most positions of virtual space with the spikerate corresponding to that observed at the maximum of RAFs recorded with natural virtual stimuli. No statistical test was conducted to show significant differences between RAFs and FixT tuning curves. Since all RAF's of units taken into account were classified as "tuned" according to the Kruskal-Wallis test in contrast to the respective FixT tuning curves, which were classified as "not tuned", a significant difference of tuning to the two stimuli is evident.

Typical RAFs for natural virtual stimuli and FixT stimuli for a so-called "low-frequency" unit classified as "not tuned" in the azimuthal range from –160° to 160° (A) and for a "high-frequency" unit not tuned in the range of –90° to 90° (B) are shown in Fig. 3.6. The azimuthal tuning of units with frequencies below 5000 Hz ("low-frequency") showed a disruption of their tuning properties over the whole tested azimuth range when stimulated with FixT stimuli. In contrast, not all high-frequency units responded over the whole azimuth rage with the spikerate observed at

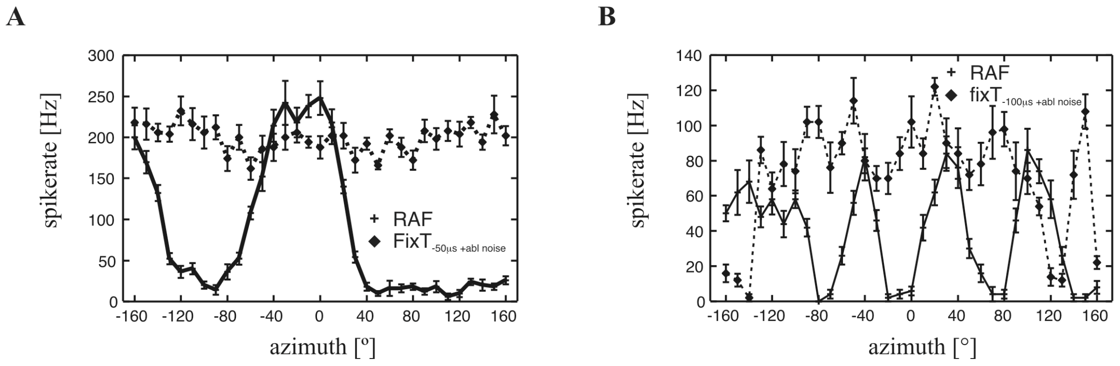

Fig. 3.6 RAFs of two ICc-core units for natural (crosses) and manipulated (diamonds) virtual stimuli. **A** Unit was classified as "not tuned" for ϕ –160° to 160° (Kruskal-Wallis, $p<0.05$) when stimulated with FixT $_{-50\mu s\ +abl\ noise}$. The unit's best frequency was at 1600 Hz ("low-frequency" unit). Mean spontaneous activity: 36.1±4.0 Hz. **B** Typical "high-frequency unit with best frequency at 5200 Hz, "not tuned" for ϕ –90° to 90° (Kruskal-Wallis, $p<0.05$) when stimulated with FixT $_{-100\mu s\ +abl\ noise}$. Mean spontaneous activity: 4.2±1.3 Hz.

Tab. 3.2 Categorization of ICc-core units according to their tuning response to the four subtypes of FixT virtual stimuli tested from ϕ –160° to 160°. 15 units (see FixT $_{\text{+abl 1/6 octave}}$) were tested with all four FixT subtypes. These units showed the same tendency in their response distribution to the four FixT subtypes as they were found for the other units.

Stimulus type / Tuning type	FixT $_{\text{-abl noise}}$	FixT $_{\text{+abl noise}}$	FixT $_{\text{-abl 1/6 octave}}$	FixT $_{\text{+abl 1/6 octave}}$	All FixT subtypes
not tuned –160° to 160°	13 (52%)	13 (46%)	11 (61%)	12 (80%)	49 (57%)
tuned –160° to 160°	12 (48%)	15 (54%)	7 (39%)	3 (20%)	37 (43%)
Σ	**25**	**28**	**18**	**15**	**86**

the maximum of the RAF recorded with natural virtual stimuli. The response rate of the unit shown in Fig. 3.6 B decreased towards the periphery. This could be observed in several of the high-frequency units. Nevertheless, these units lost their tuning characteristics in the frontal part of the auditory field (ϕ –90° to 90°).

Tab. 3.2 summarizes the results for all subtypes tested with FixT virtual stimuli from ϕ –160° to 160°. 57% of all units tested with one of the four FixT subtypes lost their tuning. A comparison of the percentages of “tuned” vs. “not tuned” units for the four FixT subtypes seems to show that narrow frequency bands are more effective in disturbing the tuning properties of ICc-core units. 80% of the units tested with FixT $_{\text{+abl 1/6 octave}}$ lost their tuning over the azimuthal range from –160° to 160°. In contrast, only 46% lost their tuning characteristics when stimulated with FixT $_{\text{+abl noise}}$.

Tab. 3.3 Categorization of ICc-core units according to their tuning response to the four subtypes of FixT virtual stimuli tested from ϕ –90° to 90°. These units showed the same tendency in their response distribution to the four FixT subtypes as they were found for the other units.

Stimulus type / Tuning type	FixT $_{\text{-abl noise}}$	FixT $_{\text{+abl noise}}$	FixT $_{\text{-abl 1/6 octave}}$	FixT $_{\text{+abl 1/6 octave}}$	All FixT subtypes
not tuned –90° to 90°	17 (68%)	17 (61%)	13 (72%)	14 (93%)	61 (71%)
tuned –90° to 90°	8 (32%)	11 (39%)	5 (28%)	1 (7%)	25 (29%)
Σ	**25**	**28**	**18**	**15**	**86**

The same tendency was found for FixT $_{\text{-abl noise}}$ (52%) and FixT $_{\text{-abl 1/6-octave}}$ (61%). Nevertheless, no significant difference between FixT $_{\text{+abl noise}}$ and FixT $_{\text{+abl 1/6-octave}}$ (t-test, $p<0.01$, $R^2=0.2939$) or between FixT $_{\text{-abl noise}}$ and FixT $_{\text{-abl 1/6-octave}}$ (t-test, $p<0.01$, $R^2=0.2317$) could be found. The same was true for FixT $_{\text{-abl 1/6 octave}}$ and FixT $_{\text{+abl 1/6-octave}}$ (t-test, $p<0.01$, $R^2=0.7894$) and for the pair FixT $_{\text{-abl noise}}$ and FixT $_{\text{+abl noise}}$ (t-test, $p<0.01$, $R^2=0.3118$).

A restriction of the analysis to the frontal auditory field (ϕ -90° to 90°) showed similar tendencies (Tab. 3.3) whereby 71% of all units tested with one of the four FixT subtypes lost their tuning characteristics. 93% of all tested units lost their tuning characteristics when stimulated with FixT $_{\text{+abl 1/6 octave}}$. Again, no statistically significant difference between FixT $_{\text{+abl noise}}$ and FixT $_{\text{+abl 1/6-octave}}$ (t-test, $p<0.01$, $R^2=0.4597$) or between FixT $_{\text{-abl noise}}$ and FixT $_{\text{-abl 1/6-octave}}$ (t-test, $p<0.01$, $R^2=0.6198$) could be found

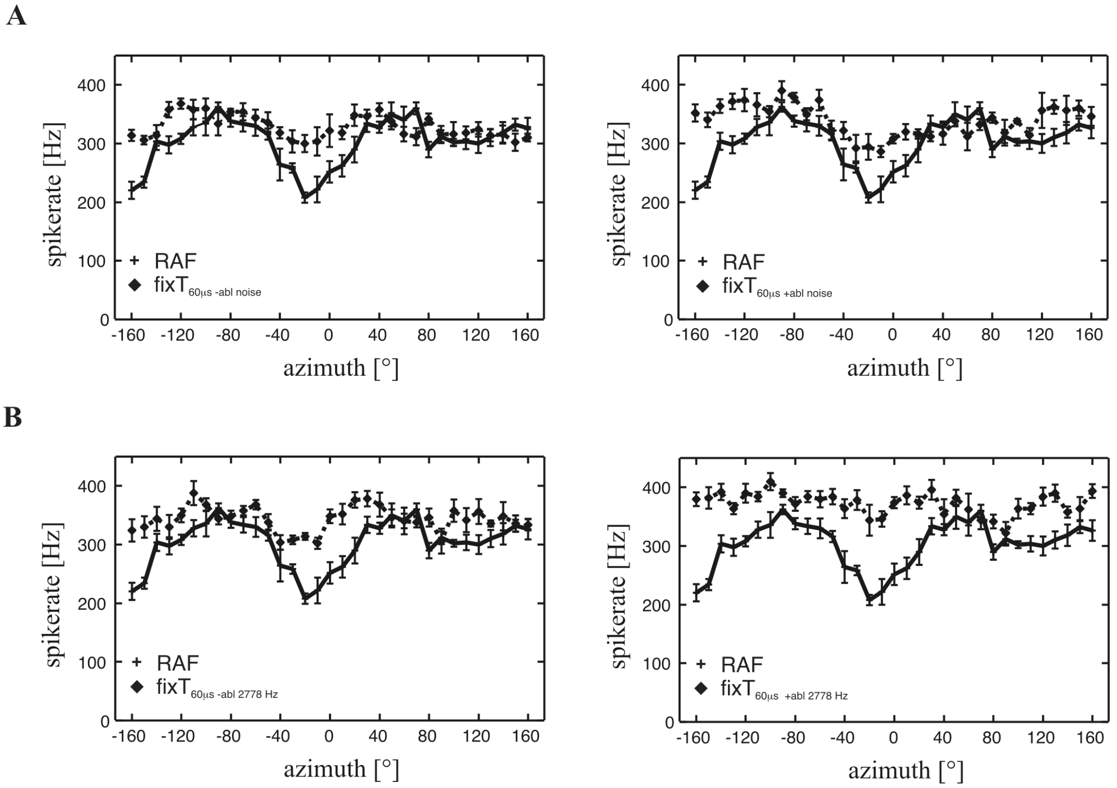

Fig. 3.7 Comparison of four different FixT stimuli. In each plot the RAF for natural virtual stimuli (crosses) is plotted together with one of the four FixT stimulus types (diamonds). In the left column FixT $_{\text{-abl}}$ is shown, in the right column FixT $_{\text{+abl}}$. Error bars indicate standard deviation. Highest mean spontaneous activity observed: 0.3±0.3 Hz. **A** According to the Kruskal-Wallis statistics both, the unit tested with FixT $_{60\mu s\ \text{-abl noise}}$ as well as that tested with FixT $_{60\mu s\ \text{+abl noise}}$ were tuned in the azimuth range from -160° to 160°. **B** The unit tested with FixT $_{60\mu s\ \text{-abl 2778 Hz}}$ was tuned (ϕ -160° to160°), that tested with FixT $_{60\mu s\ \text{+abl 2778 Hz}}$ was not tuned (ϕ -160° to160°).

The same results were obtained for FixT $_{\text{-abl 1/6 octave}}$ and FixT $_{\text{+abl 1/6-octave}}$ (t-test, $p<0.01$, $R^2=0.8624$) and for the pair FixT $_{\text{-abl noise}}$ and FixT $_{\text{+abl noise}}$ (t-test, $p<0.01$, $R^2=0.8075$).

Fig. 3.7 depicts a unit tested with all of the four FixT stimuli subtypes. Two response maxima, one at -90° and the other at around 60°, were found when tested with natural virtual stimuli. The unit's tuning was significantly disrupted when stimulated with FixT $_{+60\ \mu s\ +abl\ 2778\ Hz}$. While for the three other FixT stimuli a "dip" around -20° remained that replicated the minimum of the RAF obtained with the natural stimulus. Interestingly, a Kruskal-Wallis test that considered only the frontal space (ϕ -90° to 90°) classified the unit tested with FixT $_{\text{-abl noise}}$ as "not tuned".

3.3.4 Responses of ICc-core units to AddT stimuli

All of the 20 units tested with AddT stimuli showed a consistent behaviour. The introduction of an additional ITD led to a shift of response maximum corresponding to the ITD value as described by Eq. 3.2.

$$\text{peak shift } [°] = 6.7066 \pm 14.9° + 0.47424 \pm 0.119°/\mu s * \text{AddT } [\mu s] \qquad \text{(Eq. 3.2)}$$

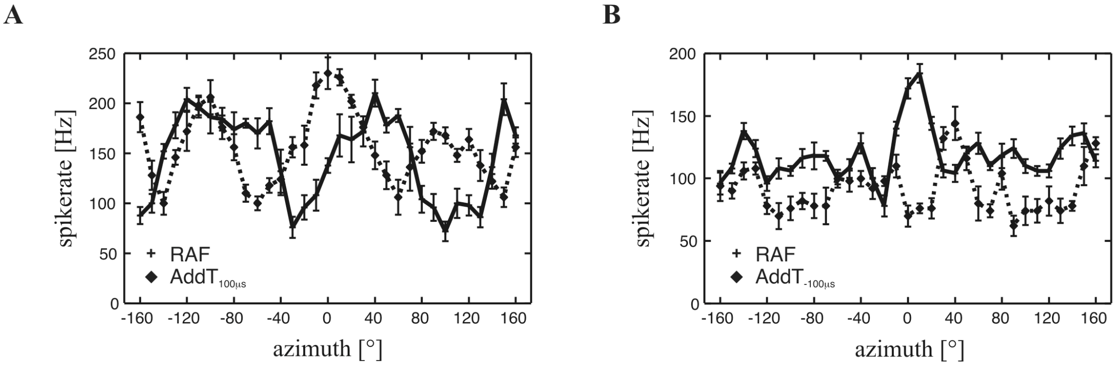

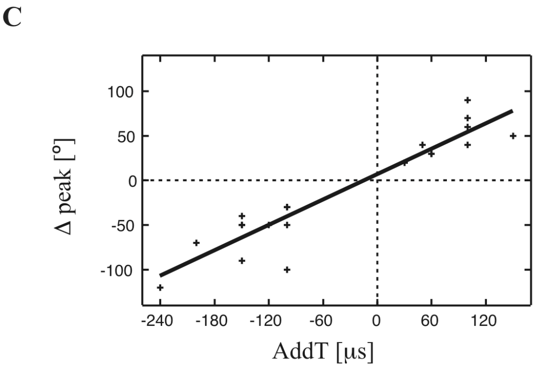

Fig. 3.8 RAFs of two ICc-core units to normal (crosses) virtual acoustic stimuli and stimuli with additional ITDs (diamonds). Error bars indicate standard deviation. **A** An additional ITD of 100 µs was introduced. Mean spontaneous activity: 5.4±1.6 Hz **B** An additional ITD of -100 µs was introduced. Mean spontaneous activity: 21.4±1.8 Hz **C** Correlation between the difference of azimuthal tuning maximum of natural and AddT RAFs and the additional ITD of AddT stimuli ($N=20$, $p<0.01$, $R^2=0.937896$).

This equation was obtained by a linear regression of the difference between the peaks of the natural and manipulated RAFs closest to 0° and the introduced additional ITD of the AddT stimuli (Fig. 3.8 C). The two parameters were positively correlated. This means, a negative AddT value shifts the peak of the RAF leftward and vice versa.

The form of the AddT tuning curves stayed very similar compared to the natural RAFs (Fig. 3.8 A, B). Interestingly, peaks around the owls centre of symmetry at about ±100° (see chapter 2) exhibited in natural RAFs that were found in several of the units were not shifted by the additional ITDs in AddT stimuli (Fig. 3.8 A).

3.3.5 Responses of ICc-ls units to dichotic and natural virtual stimuli

ICc-ls units were identified by their tuning characteristics. Units tuned to ITD and ILD (Kruskal-Wallis test; $p<0.05$) that showed phase ambiguity and a narrow frequency tuning were classified as belonging to ICc-ls. Since in ICc-ls ILD as well as ITD information is represented these units were expected to exhibit complex tuning responses to FixT and AddT stimuli. Therefore, no attempts were made to actively find ICc-ls. ICc-ls units only were recorded when encountered during the search for ICc-core.

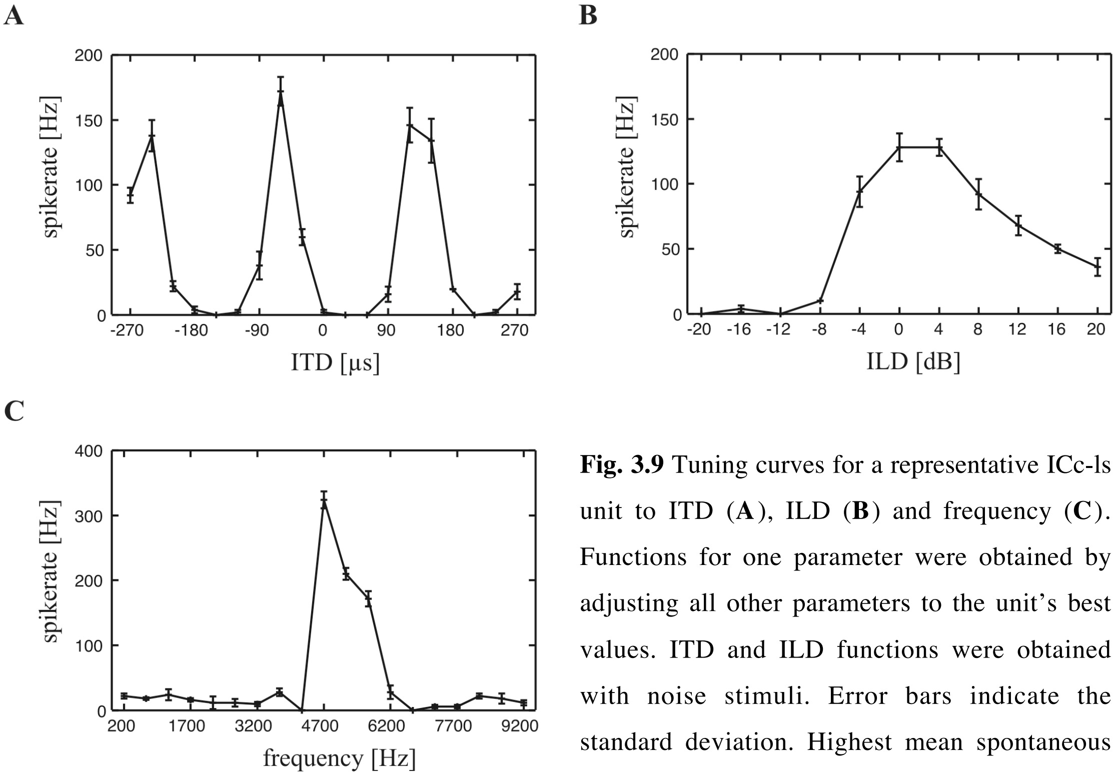

Fig. 3.9 Tuning curves for a representative ICc-ls unit to ITD (**A**), ILD (**B**) and frequency (**C**). Functions for one parameter were obtained by adjusting all other parameters to the unit's best values. ITD and ILD functions were obtained with noise stimuli. Error bars indicate the standard deviation. Highest mean spontaneous activity observed: 14.3±1.8 Hz

Fig. 3.9 depicts a typical ICc-ls unit. The unit exhibited a cyclic response to ITD (Fig. 3.9 A) and a period of 180 μs suggesting a best frequency of 5556 Hz. The recorded best frequency was 4700 Hz as can be seen in Fig. 3.9 C. The unit was sensitive over a wide range of ILDs as is typical for ICc-ls (Fig. 3.9 B). Another characteristic of ICc-ls units were their response to monaural RLFs. While the RLF for the ear contralateral to the recording site was comparable to that of ICc-core units, RLFs for the ipsilateral ear were inhibited (data not shown).

3.3.6 Responses of ICc-ls units to FixT and AddT stimuli

As noted above ICc-ls units were recorded when encountered during the search for ICc-core. Therefore, only 17 units were recorded of which 11 were tested with FixT stimuli. 8% of these units tested lost their tuning to azimuth from ϕ –160° to 160° (Tab 3.5; Kruskal-Wallis test; $p<0.05$). A restriction to the frontal auditory space (ϕ –90° to 90°; Tab 3.6) led to a loss of tuning properties in 29% of the neurons tested. No statistics were made to analyse the ICc-ls units any further. Most units showed a complex response pattern to FixT stimuli (Fig. 3.10 A). Tuning could be disrupted in only a few of the tested units (Fig. 3.10 B).

All of the encountered 17 units were tested with AddT stimuli. Their response to these stimuli was inconsistent (Fig. 3.11). Three units did not respond to the additional ITD at all. Peak and shape of the natural and manipulated RAF remained the same (black circles in Fig. 3.11 D). Two of the tested units exhibited an inverse-linear relation (black diamonds in Fig. 3.11 D). The rest of the units that were used for

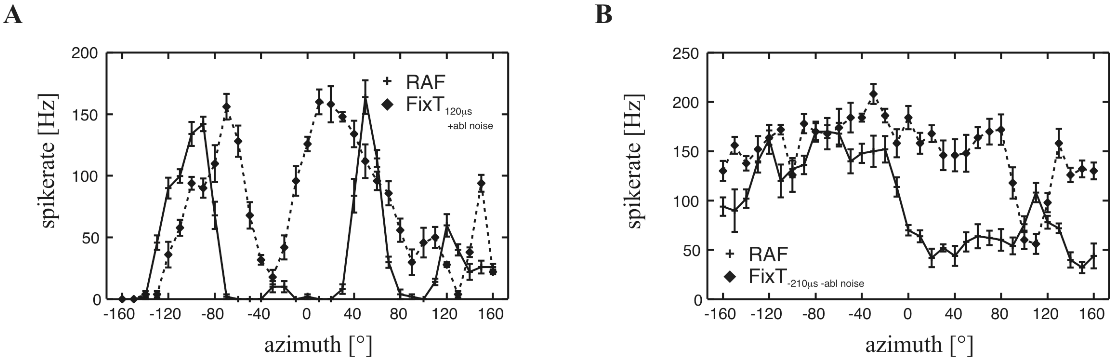

Fig. 3.10 RAFs for natural (crosses) and FixT stimuli (diamonds) for two ICc-ls units. Error bars indicate standard deviation. **A** Unit showed complex response behaviour to FixT $_{120\mu s\ +abl\ noise}$. Mean spontaneous activity: 16.5±2.5 Hz **B** This unit tested with FixT $_{-210\mu s\ -abl\ noise}$ was tuned (ϕ –160° to 160°), but was classified as “not tuned” to ϕ – 90° to 90°. Mean spontaneous activity: 6.2±1.7 Hz

Tab. 3.5 Categorization of ICc-ls units according to their tuning response to the four subtypes of FixT virtual stimuli tested from ϕ –160° to 160°.

Stimulus type Tuning type	FixT $_{-abl}$ noise	FixT $_{+abl}$ noise	FixT $_{-abl}$ 1/6 octave	FixT $_{+abl}$ 1/6 octave	All FixT subtypes
not tuned –160° to 160°	0 (0%)	2 (18%)	0 (0%)	0 (0%)	2 (8%)
tuned –160° to 160°	11 (100%)	9 (82%)	1 (100%)	1 (100%)	22 (92%)
Σ	**11**	**11**	**1**	**1**	**24**

Tab. 3.6 Categorization of ICc-ls units according to their tuning response to the four subtypes of FixT virtual stimuli tested from ϕ –90° to 90°.

Stimulus type Tuning type	FixT $_{-abl}$ noise	FixT $_{+abl}$ noise	FixT $_{-abl}$ 1/6 octave	FixT $_{+abl}$ 1/6 octave	All FixT subtypes
not tuned –90° to 90°	5 (45%)	2 (18%)	0 (0%)	0 (0%)	7 (29%)
tuned –90° to 90°	6 (55%)	9 (82%)	1 (100%)	1 (100%)	17 (71%)
Σ	**11**	**11**	**1**	**1**	**24**

regression analysis showed behaviour similar to that found for the ICc-core units. A linear relationship between the shift of maximum response and the introduced additional ITD was found that could be expressed by equation 3.3.

$$\text{peak shift } [^\circ] = 0.38458 \pm 7.65^\circ + 0.37822 \pm 0.073^\circ/\mu\text{s} * \text{AddT } [\mu\text{s}] \quad \text{(Eq. 3.3)}$$

3.4 Discussion

The results of the present chapter demonstrate that azimuthal tuning of ICc-core neurons is successfully disrupted when stimulated with manipulated virtual acoustic stimuli. The RAF became flat when fixing the ITD to the unit's best value while all other spatial cues remained unaltered. Thus, ITD is the main parameter influencing the azimuhal tuning in ICc-core units.

In contrast to this, azimuthal tuning of ICc-ls units could not be disrupted successfully. This indicates that in addition to ITD another parameter – supposedly ILD – influences the tuning properties of these units.

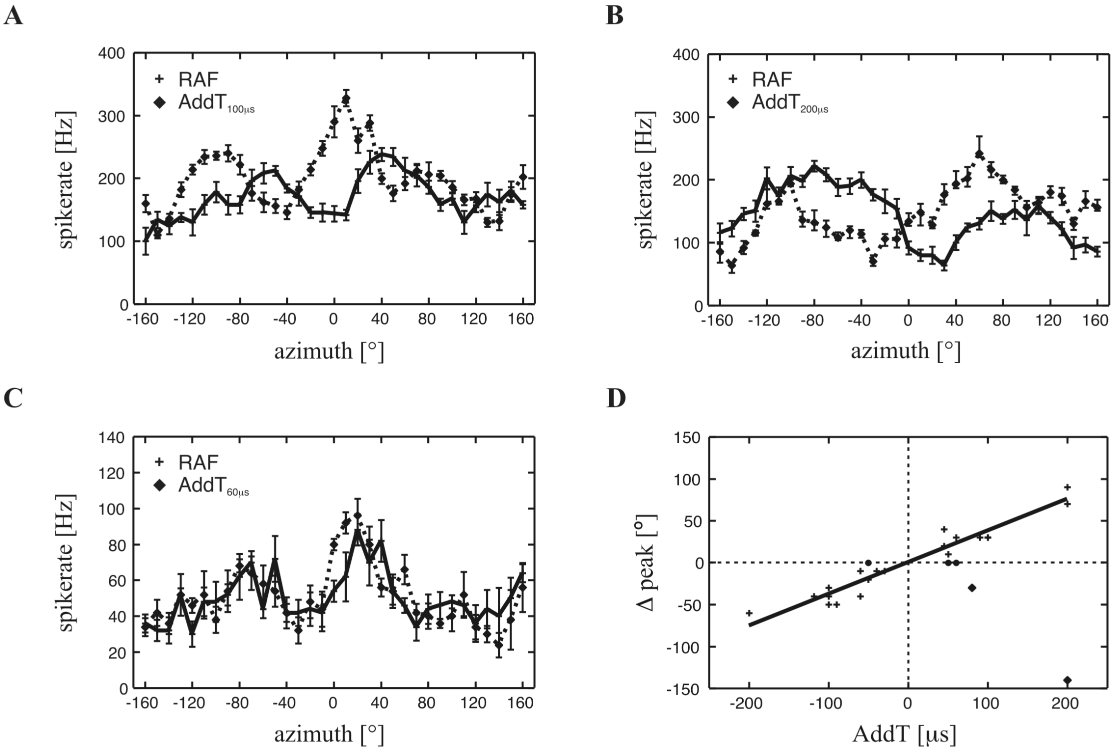

Fig. 3.11 RAFs of three ICc-ls units to normal (crosses) virtual acoustic stimuli and stimuli with additional ITDs (diamonds). Error bars indicate standard deviation. **A** An additional ITD of 100 µs was introduced. The response maximum shifted by 30° from 40° to 10°. This is typical for units exhibiting linear correlation between ITD and azimuth. ITD maximum: 100 µs. Mean spontaneous activity: 1.1±0.7 Hz **B** An additional ITD of 200 µs was introduced. The response maximum shifted from –80° to 60° exhibiting an inverse correlation. ITD maximum: – 270 µs. Mean spontaneous activity: 5.0±1.1 Hz **C** An additional ITD of 60 µs was introduced. The response peak of the unit did not shift. ITD maximum: 60 µs. Mean spontaneous activity: 2.9±01.3 Hz **D** A linear correlation between the difference of azimuthal tuning maximum of natural and AddT RAFs and the additional ITD of AddT stimuli for several of the ICc-ls units was found (N=19, $p<0.01$, $R^2=0.964308$). The regression line was calculated using data indicated by crosses. Note that three units did not respond to AddT stimuli (black circles) while two exhibited an inverse linear correlation (black diamonds).

Furthermore, it was possible to replicate the linear correlation between ITD and azimuth, as it is known from free-field studies for midbrain neurons (Olsen et al. 1989). The reciprocal value of the slope of 2.57 µs/° (see Eq. 3.1) corresponds well with that found in literature (Olsen free-field: 2.31 and 2.52 µs/°; Poganiatz VAS: 2.8 µs/°). This, together with the obvious similarities of the tuning properties found in this study and those from literature, underlines the equivalence of free-field and VAS stimulation for use in electrophysiological experiments in the owl. At the same time this confirms that no methodical errors were introduced by the VAS stimulation.

3.4.1 The influence of FixT stimuli on azimuthal tuning in IC

ITD and ILD are separately represented in the ascending auditory pathway of the owl. This was described in section 3.1.1. The last station in the time pathway in which time without intensity is coded is ICc-core (Wagner et al. 1987; Takahashi et al. 1989; Wagner et al. 2002). There, neurons exhibit a cyclic response to ITD or IPD without being sensitive to ILD (Wagner et al. 1987; Fujita and Konishi 1991; Wagner et al. 2002). In contrast, a fixation of ITD to the neurons best ITD when stimulated with virtual acoustic stimuli leads to a flat response (Poganiatz 2000). Moreover, these neurons are sharply tuned to frequency (Knudsen and Konishi 1978) and therefore, their response to frequency-specific IPD and broadband ITD are similar. All of these characteristics demonstrate the representation of IPD in ICc-core. This could be confirmed in the present study. A disruption of azimuthal tuning was observed in ICc-core, when units were stimulated with virtual acoustic stimuli whose ITD was fixed to the units' best value. The stimulus paradigm used allowed the disruption of tuning in 71% of all units in the range from ϕ –90° to 90°. This range could be extended to ϕ –160° to 160°, whereby 57% of the units tested lost their tuning properties. This indicates that ITD was the only spatial cue influencing azimuthal tuning in those units. This influence on tuning was especially obvious in low-frequency units (Fig. 3.6). ILD changes less for those frequencies and – in addition – air attenuates lower frequencies less than higher ones. Accordingly, in low frequency neurons under natural conditions ITD is the prominent cue already.

In contrast to ICc-core, in ICc-ls ITD and ILD are represented (Fujita and Konishi 1991; Adolphs 1993). Accordingly, a fixation of ITD to the unit's best value in virtual acoustic stimuli did not lead to a total disruption of tuning (Fig. 3.10). This is indicative of another parameter influencing azimuthal tuning in this subdivision of the IC. It is likely that this additional parameter is ILD. On the other hand it is possible that monaural and binaural frequency-specific cues influence the tuning properties. This could be shown for auditory OT neurons (Gold and Knudsen 1999, 2000). Thus, for ICc-ls neurons a final conclusion cannot be drawn from the present dataset.

3.4.2 Comparison of the four different FixT subtypes for ICc-core

The comparison of the four subtypes of FixT stimuli for ICc-core showed that most units lost their tuning properties when stimulated with FixT $_{\text{+abl 1/6-octave frequency band}}$. 93% of all tested units lost their tuning characteristics in the range from ϕ –90° to 90° (Tab. 3.3). The extension to ϕ –160° to 160° led to a loss in 80% of the units (Tab 3.2). The response rate to stimuli with identical overall level decreases towards the periphery of auditory space. This is due to the mentioned directionality of the owl's facial ruff. Accordingly, stimuli that were balanced for this decrease in a frequency-specific manner were expected to lead to a disruption of tuning over the whole tested azimuth range. As mentioned above, ICc-core neurons are sharply tuned to frequency. Therefore, an optimal virtual stimulus for the here examined question would be a narrow frequency band centred at the unit's best frequency with ABL-correction. Interestingly, no statistically significant difference between FixT $_{\text{+abl 1/6-octave frequency band}}$ and FixT $_{\text{-abl 1/6-octave frequency band}}$ was found. This is probably attributable to the small number of units available for the respective FixT subtype. Nevertheless, less units (ϕ –160° to 160°: 61% Tab 3.2; ϕ –90° to 90°: 72% Tab. 3.3) lost their tuning properties when presented stimuli without ABL-correction.

In contrast to this finding, the opposite relation was found for FixT $_{\text{+abl noise}}$ and FixT $_{\text{-abl noise}}$. For both azimuth ranges more units lost their tuning to noise stimuli without ABL-correction. This could be due to influences from other neurons that were stimulated more effectively by the ABL-corrected broadband noise. One possible explanation could be the influence of GABA-ergic inhibition (Fujita and Konishi 1991). But since the investigation of inhibition with specific antagonists like bicuculline methiodide is not easily accomplished and lies beyond the scope of this thesis, a definitive answer to this unexpected finding could not be given.

To summarize this, stimulation with a narrow frequency band with ABL-correction was most efficient in disrupting the tuning properties of ICc-core units. This is due to the narrow frequency tuning in ICc-core and the correction of the spatial attenuation by the ABL-factors. When stimulated with broadband noise with ABL-correction less units lost their tuning properties compared to noise stimulation without ABL-correction. A possible explanation for this finding might be the influence of neurons stimulated by other frequencies contained in the noise.

3.4.3 The influence of AddT stimuli on azimuthal tuning in IC

Like the results obtained for ICc-core with FixT stimuli, AddT stimuli suggest a similar importance of ITD for azimuthal tuning. The additional ITD caused only a shift of the response maximum without altering the shape of the function. Again, this is evidence for the influence of ITD on the tuning properties of these neurons. The units exhibited a linear relation between additional ITD and peak shift (Eq. 3.2). The inverse of the slope (2.11 μs/°) of the corresponding regression line was in good accordance with the above mentioned slope values of ITD/azimuth correlations. This implies that ITD is one of the important cues that are responsible for azimuthal tuning in ICc-core (2.64 μs/°; Eq. 3.3).

This held not true for all of the ICc-ls units tested. The majority of the units tested showed a linear correlation (2.64 μs/°; Eq. 3.3). It is, however, noteworthy that two of the ICc-ls units showed an inverse linear correlation. The one unit was tested with an AddT stimulus that would shift the response peak beyond the owl's symmetry centre at about ϕ ±100° (Fig. 3.11 B). The resulting peak was neither correlated with the period of the unit's frequency (3700 Hz → 270 μs) nor with the introduced additional ITD of 200 μs. Interestingly, this unit's ITD maximum (–270 μs) was outside the physiological range of the owl. This finding could help verify the existence of a centre of symmetry electrophysiologically. It is thinkable that a series of experiments conducted in ICc could help to underline the here presented data by systematically trying to shift the response maximum beyond the anatomical centre of symmetry. The second unit that exhibited an inverse correlation responded best to a frequency of 7700 Hz. This corresponded good to the period of 150 μs calculated from the ITD curve. There was nothing else noteworthy about this unit that could explain the deviation in response to the AddT stimulus. Therefore, it would be necessary to record more units in ICc-ls to establish a solid data basis.

Three units did not respond to the additional ITD at all (Fig. 3.11 C). Their response characteristics stayed virtually the same in comparison with not manipulated virtual stimuli. It is possible that this behaviour is an artefact due to under-sampling. On the other hand it is thinkable that this is due to statistical variance. Again, since the data basis is rather small a conclusion cannot be drawn from this limited set of data.

3.4.4 Conclusion

The data presented in this chapter gives good evidence for the main importance of ITD on azimuthal coding in ICc-core. In contrast, in ICc-ls other parameters not yet identified contribute to the coding of azimuth. Most ICc-core units were effectively disrupted when stimulated with FixT $_{\text{+abl 1/6 ocatve}}$. However, it was not possible to find a statistically significant difference between any of the four FixT subtypes tested, although the contrary was anticipated. This was due to the limited size of data sampled. In addition, it turned out that more units lost their tuning characteristics when presented with FixT $_{\text{-abl noise}}$ compared to the stimulation with ABL-correction. The reason for this behaviour could not be found. To further elucidate these unexpected findings more experiments should be conducted to enlarge the data basis.

Nevertheless, it could be shown that the VAS technique is an appropriate means to simulate free-field, since no differences in the neurons' tuning characteristics between this study and free-field studies were found. In addition to this, a comparison of slope values yielded by linear correlation of ITD and azimuth functions from this study and literature, showed convincing similarity.

3.5 References

Adolphs (1993) Bilateral inhibition generates neuronal responses tuned to interaural level differences in the auditory brainstem of the barn owl. *J. Neurosci.* 13: 3647-3668

du Lac S and Knudsen EI (1990) Neural maps of head movement vector and speed in the optic tectum of the barn owl. *J. Neurophysiol.* 63: 131-146

Euston DR and Takahashi TT (2002) From spectrum to space: The contribution of level difference cues to spatial receptive fields in the barn owl inferior colliculus. *J. Neurosci.* 22: 284-293

Fujita I and Konishi M (1991) The role of GABAergic inhibition in processing of interaural time difference in the owl's auditory system. *J. Neurosci.* 11: 722-739

Gold JI and Knudsen EI (1999) Hearing impairment induces frequency-specific adjustments in auditory spatial tuning in the optic tectum of young owls. *J. Neurophysiol.* 82: 2197-2209

Gold JI and Knudsen EI (2000) Abnormal auditory experience induces frequency-specific adjustments in unit tuning for binaural localization cues in the optic tectum of juvenile owls. *J. Neurosci.* 20: 862-877

Jeffress LA (1948) A place theory of sound localization. *J. Comp. Physiol. Psychol.* 41: 35-39

Knudsen EI and Konishi M (1977) A neural map of auditory space in the owl. *Science* 200:795-797

Knudsen EI and Konishi M (1978) Space and frequency are represented separately in auditory midbrain of the owl. *J.Neurophysiol.* 41: 870-884

Knudsen EI (1982) Auditory and visual maps of space in the optic tectum of the owl. *J. Neurosci.* 2: 1177-1194

Knudsen EI and Knudsen PF (1983) Space-mapped auditory projections from the inferior colliculus to the optic tectum in the barn owl (*Tyto alba*). *J. Comp. Neurol.* 218: 187-196

Knudsen EI (1984) Auditory properties of space-tuned units in owl's optic tectum. *J.Neurophysiol.* 52: 709-723

Konishi M (2003) Coding auditory space. *Annu. Rev. Neurosci.* 26:31-55

Masino T and Knudsen EI (1990) Horizontal and vertical components of head movement are controlled by distinct neural circuits in the barn owl. *Letters to Nature* 345: 434-437

Mazer JA (1998) How the owl resolves auditory coding ambiguity. *Proc. Natl. Acad. Sci. USA* 95:10932-10937

Miller GL and Knudsen EI (1999) Early visual experience shapes the representation of auditory space in the forebrain gaze fields of the barn owl. *J. Neurosci.* 19: 2326-2336

Moiseff A and Konishi M (1983) Binaural characteristics of units in the owl's brainstem auditory pathway: precursors of restricted spatial fields. *J. Neurosci.* 3: 2553-2562

Olsen JF, Knudsen EI, Esterly SD (1989) Neural maps of interaural time and intensity difference in the optic tectum of the barn owl. *J. Neurosci.* 9: 2591-2605

Parks TN, Rubel EW (1975) Organization and development of brain stem auditory nuclei of the chicken: Organization of projections from N. magnocellularis to N. laminaris. *J. Comp. Neurol.* 164: 435-448

Peña JL, Viete S, Albeck Y and Konishi M (1996) Tolerance to sound intensity of binaural coincidence detection in the nucleus laminaris of the owl. *J. Neurosci.* 16: 7046-7054

Peña JL and Konishi M (2000) Cellular mechanisms for resolving phase ambiguity in the owl's inferior colliculus. *Proc. Natl. Acad. Sci. USA* 97: 11787-11792

Poganiatz I (2000) Sound-localization in barn owls – Experiments with virtual space stimuli – *PhD-Thesis at the Reihnisch-Westfälische Technische Hochschule Aachen*

Poganiatz I, Nelken I, Wagner H (2001) Sound-localization experiments with barn owls in virtual space: influence of interaural time difference on head-turning behavior. *J. Assoc. Res. Otolaryngol.* 2: 1-21

Sullivan WE and Konishi M (1986) Segregation of stimulus phase and intensity in the cochlear nuclei of the barn owl. *J. Neurosci.* 4:1786-1787

Takahashi TT and Konishi M (1986) Selectivity for interaural time difference in the owl's midbrain. *J. Neurosci.* 6: 3413-3422

Takahashi TT, Wagner H, Konishi M (1989) Role of commissural projections in the representation of bilateral auditory space in the barn owl's inferior colliculus. *J. Comp. Neurol.* 281: 545-554

Takahashi TT, Bala ADS, Spitzer MW, Euston DR, Spezio ML, Keller CH (2003) The synthesis and use of the owl's auditory space map. *Biol. Cybern.* 89: 378-387

Wagner H, Takahashi T, Konishi M (1987) Representation of interaural time difference in the central nucleus of the barn owl's inferior colliculus. *J. Neurosci.* 7: 3105-3116

Wagner H, Mazer JA, von Campenhausen M (2002) Response properties of neurons in the core of the central nucleus of the inferior colliculus of the barn owl. *Europ. J. Neurosci.* 15: 1343-1352

Chapter 4

General Discussion

The present thesis described the measurement of HRTFs of barn owls, the calculation of virtual acoustic stimuli for the use in electrophysiological experiments and studied the influence of ITD on azimuthal coding in ICc-core neurons. In this chapter the findings will be summarized and put into context with other findings. In addition, ideas for future experiments with virtual acoustic space stimuli will be given. This should help to achieve a broader understanding of the importance of ITD for sound localization in owls.

4.1 Summary and discussion of the obtained results

The spatial pattern of broadband ITD as calculated from HRIRs demonstrated a linear change of ITD with azimuth over the whole range tested (Fig. 2.2). Hence, ITD seems to be an appropriate cue for coding azimuth. The relation between ITD and azimuth became as well apparent electrophysiologically. A linear correlation between the response maximum of ITD functions and that of rate-azimuth functions was found in ICc-core. This indicated the importance of ITD as the main parameter that influences coding of azimuth in the owl’s midbrain. The value for the slope of the regression line obtained in this study (Eq. 3.1) was in good coherence with literature (Olsen et al. 1989; Poganiatz 2000). The same linear correlation was found for ICc-core neurons stimulated with AddT stimuli. In this case the shift of the response maximum was linearly correlated with the introduced additional ITD (Eq. 3.2). The slope yielded was in coherence with literature as well (Olsen et al. 1989; Poganiatz 2000). This coherence demonstrated that no errors were introduced by the virtual space technique. The major problem in VAS is not the insertion depth of the microphones but the correct placement of earphones on each experiment. Keller et al. (1998) demonstrated that the last few millimetres of the owl's ear canal do not have a major influence on the directional filtering. Instead, the largest errors arise due to slightly different placement of the earphones. Nevertheless, off-line analysis of reference measurements with repeatedly applied earphones showed no significant differences. Therefore, the influence of earphone placement could be neglected.

The results obtained with manipulated virtual acoustic stimuli, especially of the FixT type, clearly demonstrated that for ICc-core neurons ITD mainly influences azimuthal tuning. To disrupt a neuron's tuning characteristics over the whole azimuthal range it was important to design the stimulus in a proper manner. ICc-core neurons are sharply tuned to frequency. Therefore, narrow frequency band stimuli centred at the neuron's best frequency were considered to be better suited for this kind of experiment than broadband noise stimuli. In addition, the effects of attenuation in the rear hemisphere due to the high directionality of the owl's ruff were taken into account by the application of ABL-correction factors that compensated for the decrease in average binaural level. Accordingly, 93% of all units tested with those FixT stimuli lost their tuning characteristics over the frontal range (ϕ –90° to 90). Still 80% of the units were not tuned over the whole range tested (ϕ –160° to 160). Consequently, narrow frequency stimuli without ABL-correction led to a loss of tuning in fewer units (ϕ –160° to 160: 61%; ϕ –90° to 90: 72%). Nevertheless, no statistically significant difference between the two stimuli subtypes was found.

The opposite relation was observed for broadband FixT stimuli. In both azimuth ranges more units could be disrupted with FixT stimuli lacking ABL-correction (ϕ –160° to 160: $\text{FixT}_{\text{-abl noise}}$ 52%, $\text{FixT}_{\text{+abl noise}}$ 46%; ϕ –90° to 90: $\text{FixT}_{\text{-abl noise}}$ 68%, $\text{FixT}_{\text{+abl noise}}$ 61%). Nevertheless, again no significant difference between both stimuli types was found. ILD as a parameter that influences the tuning of the units may be excluded, since ICc-core neurons are not tuned to ILD. A possible explanation of this finding could be the influence of inhibitory input. GABAergic inhibition plays a role in sharpening the ITD response curves in the cochlea nuclei (Fujita and Konishi 1991). Due to the broadband stimulation a large number of excitatory and inhibitory neurons with different best frequencies from the same iso-frequency lamina or neighbouring laminae were activated. These neurons – either from the ipsi- or contralateral site – could have an inhibitory influence that leads to a decrease in the ICc-core neurons' activity that was observed. To assess this influence experiments with antagonists that block inhibitory neurotransmitters must be conducted. This is out of scope of the present thesis but could be one of the possible follow-up experiments. Another possible reason could be cross talk through the auditory channel (Coles and Guppy 1988) that is most prominent for low frequencies.

Generally, the loss of tuning over the whole azimuthal range tested was particularly obvious in low-frequency units (Fig. 3.6). The response rate of high-frequency units tended to decrease towards the periphery. The reason for this could be that ILD changes less for low frequencies and – in addition – air attenuates lower frequencies less than higher ones. Accordingly, for low frequencies under natural conditions ITD is the prominent cue already. In humans a dominance of low-frequency cues for localization in azimuth was found (Hartmann and Wittenberg 1996; Wightman and Kistler 1992). Such a separation of low frequencies for azimuthal and high frequencies for elevational localization is not true for the owl. It could be demonstrated electrophysiologically that IPDs are processed up to 9 kHz (Sullivan and Konishi 1984; Köppl 1997). In addition with behavioural studies (Moiseff 1989; Poganiatz 2001) and the fact that ITD is fairly independent of frequency (von Campenhausen personal communication), the results of the present study are consistent with the hypothesis that in ICc-core azimuth tuning of neurons is almost exclusively influenced by ITD.

Although this is true for ICc-core where only ITD is represented, space-specific neurons in ICx and OT reveal a more complex dependence of ITD and ILD, which contribute to the formation of a 2-D receptive field in those neurons (Poganiatz 2000; Euston and Takahashi 2002). Poganiatz (2000) employed a similar paradigm to that used in the present thesis to study the characteristics of those neurons. The response of ICx and OT neurons to FixT stimuli was tested. In contrast to the present study, ABL was not fixed. Only one third of the units tested showed a flat response over the whole azimuthal range tested (ϕ –140° to 140°). The other units exhibited a complex behaviour similar to that found for ICc-ls units in this study. This suggests the importance of other parameters for coding of azimuth and thus for the formation of the 2-D receptive fields in those space-specific neurons. Since in the study of Poganiatz no ABL-correction was employed these results should be considered preliminary. Nevertheless, a study with ABL-correction by Euston and Takahashi (2002) showed that both ITD and ILD contribute to the formation of receptive fields in ICx. Even though ILD varies with azimuth for frequencies below 4 kHz and could therefore define a receptive field on its own, ITD is necessary for the formation of a 2-D receptive field. ITD contributes the horizontal and ILD the vertical component to the formation of a neuron's receptive field. Yet, in addition Euston and Takahashi (2002) made a model predicting so-called ILD-alone receptive fields (e.g. only parameter that changes is ILD). They compared recorded broadband ILD-alone receptive fields with receptive fields created by summing up the responses to frequency-specific inputs. This is based on the knowledge that ICx neurons integrate over the whole relevant frequency range to eliminate the phase-ambiguous input from ICc-core. They were able to account for 56% of the variance in their recorded broadband ILD-alone receptive fields. Hence, the simple distinction between ITD as sole cue for coding azimuth and ILD as sole cue for coding elevation is not possible in space-specific neurons.

This is an interesting finding since in ICc-core ITD is directly correlated to azimuth. At least for narrow frequency band stimuli there is no evidence that another parameter influences the tuning to azimuth in the frontal hemisphere. Obviously, additional information is processed to create a receptive field in ICx and OT. This additional information is probably not processed in the ITD part of the ascending auditory pathway but more likely in the ILD part (Sullivan and Konishi 1984; Takahashi et al. 1984). The HRTF measurement clearly demonstrated a linear relation of ITD and azimuth. This relation was more complex for ILD and elevation. In fact ILD changes in a frequency-dependent way as described earlier. Therefore, a more complex influence of ILD on the formation of receptive fields should be anticipated.

Yet, even less is known about the contribution of monaural cues on coding of azimuth in those space-specific neurons. VAS is the ideal method to investigate this influence in detail. It is possible to carefully manipulate the monaural amplitude spectra by, for example, introducing additional notches to one ear or deleting them in the other ear. Of course this manipulation has to be done very carefully since such a monaural manipulation also changes ILD. If monaural cues play no role in the definition of the azimuthal component of the receptive field the tuning of ICc-core, ICx or OT neurons should be the same for normal and manipulated stimuli.

Only a limited number of units were recorded in ICc-ls. Therefore, a detailed analysis and discussion is not possible. Nevertheless, one finding should be noted. Two units tested with AddT stimuli exhibited an inverse linear correlation between ITD and azimuth. This finding cannot be explained at the moment. It is obvious that more units must be sampled in ICc-ls to come to a final conclusion about the significance of this finding. However, one issue remains. One of those two units the additional ITD would have shifted the response peak beyond the owl's centre of symmetry at about –100° azimuth (Fig. 3.11 B). A peak at ϕ –100° remained and an additional one appeared ϕ 60°. It was not possible to relate that additional peak of response to either the introduced ITD or the period of the unit. A peak at ϕ ±100° that could not be shifted was observed in several of the units tested with AddT stimuli. Therefore, it is thinkable that this peak is related to the centre of symmetry. A series of experiments that tries to shift the response maximum beyond this centre of symmetry could reveal a systematic correlation in either ICc-core or ICc-ls units. This would then be a supplementary electrophysiological evidence supporting the evidence from HRTF-measurements (see chapter 2) for a centre of symmetry at ϕ ±100° in the owl.

Thus, taking this altogether, the present study provided data in accordance with the current hypothesis that ITD is the main parameter to influence the azimuth tuning in the barn owl.

4.2 References

Coles RB and Guppy A (1988) Directional hearing in the barn owl (*Tyto alba*). *J. Comp. Physiol A* 163: 117-133.

Euston DR and Takahashi TT (2002) From spectrum to space: The contribution of level difference cues to spatial receptive fields in the barn owl inferior colliculus. *J. Neurosci.* 22: 284-293

Fujita I and Konishi M (1991) The role of GABAergic inhibition in processing of interaural time difference in the owl's auditory system. *J. Neurosci.* 11: 722-739

Hartmann WM and Wittenberg A (1996) On the externalization of sound images. *J. Acoust. Soc. Am.* 99: 3678-3688

Keller CH, Hartung K, Takahashi TT (1998) Head-related transfer functions of the barn owl: measurement and neural responses. *Hear. Res.* 118: 13-34

Köppl C (1997) Phase locking to high frequencies in the auditory nerve and cochlear nucleus magnocellularis of the barn owl, *Tyto alba*. *J. Neurosci.* 17: 3312-3321

Moiseff A (1989) Bi-coordinate Sound Localization by the Barn Owl. *J. Comp. Physiol. A* 164: 637-644

Olsen JF, Knudsen EI, Esterly SD (1989) Neural maps of interaural time and intensity difference in the optic tectum of the barn owl. *J. Neurosci.* 9: 2591-2605

Poganiatz I (2000) Sound-localization in barn owls – Experiments with virtual space stimuli – *PhD-Thesis at the Reihnisch-Westfälische Technische Hochschule Aachen*

Poganiatz I, Nelken I, Wagner H (2001) Sound-localization experiments with barn owls in virtual space: influence of interaural time difference on head-turning behavior. *J. Assoc. Res. Otolaryngol.* 2: 1-21

Sullivan WE and Konishi (1984) Segregation of stimulus phase and intensity coding in the cochlear nucleus of the barn owl. *J. Neurosci.* 4: 1787-1799

Takahashi T, Moiseff A, Konishi M (1984) Time and intensity cues are processed independently in the auditory system of the owl. *J. Neurosci.* 4: 1781-1786

Wightman FL and Kistler DJ (1992) The dominant role of low-frequency interaural time differences in sound localization. *J. Acoust. Soc. Am.* 91: 1648-1661

5. Abbreviations

ABL	average binaural level
AddT$_x$	manipulated virtual stimuli with additional inter aural time difference with x denoting the additional ITD
FixT$_{x\ \text{-abl noise}}$	virtual stimuli with fixed interaural time difference at x µs, without correction for the average binaural level and stimulated with broadband noise
FixT$_{x\ \text{+abl noise}}$	virtual stimuli with fixed interaural time difference at x µs, with correction for the average binaural level and stimulated with broadband noise
FixT$_{x\ \text{-abl 1/6-octave frequency band}}$	virtual stimuli with fixed interaural time difference at x µs, without correction for the average binaural level and stimulated with 1/6 frequency octave band centred at the unit's best frequency
FixT$_{x\ \text{+abl 1/6-octave frequency band}}$	virtual stimuli with fixed interaural time difference at x µs, with correction for the average binaural level and stimulated with 1/6 frequency octave band centred at the unit's best frequency
HRIR	head-related impulse response
HRTF	head-related transfer function
IC	inferior colliculus
ICc	central nucleus of the inferior colliculus
ICc-core	core of the central nucleus of the inferior colliculus
ICc-ls	lateral shell of the central nucleus of the inferior colliculus
ICx	external nucleus of the inferior colliculus
ILD	interaural level difference
IR	impulse response
ITD	interaural time difference
MU	multi unit
OT	optic tectum
SU	single unit
VAS	virtual acoustic (or auditory) space
ϕ	azimuth
θ	elevation

6. Acknowledgements

Mein besonderer Dank gilt Herrn Prof. Dr. Hermann Wagner für die Überlassung des Themas und für die Übernahme des Erstreferats. Seine Betreuung besonders seine praktischen Hilfestellungen bei den elektrophysiologischen Experimenten haben maßgeblich zum Erfolg dieser Arbeit beigetragen.

Herrn PD Dr. Harald Luksch danke ich für die Übernahme des Koreferats.

Dr. Mark von Campenhausen bin ich sehr zu Dank verpflichtet für seine Hilfe bei der Durchführung der HRTF-Messungen und deren Auswertung, für die er großzügig seine MatLab-skripte zur Verfügung gestellt hat. Darüberhinaus habe ich durch seine unermüdliche Diskussionsbereitschaft sehr viel dazugelernt.

Für Unterstützung und freundlicher Anteilnahme an meiner Arbeit möchte ich Dr. Dennis T.T. Plachta sowie Dr. Rob van der Willigen danken.

Desweiteren gilt mein Dank dem gesamten Institut für Biologie II (Zoologie/Tierphysiologie) für die Hilfsbereitschaft und das gute Arbeitsklima.

Ganz herzlich möchte ich mich bei meiner Familie bedanken, die mein Studium ermöglicht und mich zu jeder Zeit ermutigt und unterstützt hat.

Hiermit versichere ich, daß ich die vorliegende Diplomarbeit selbstständig verfasst und keine anderen, als die angegebenen Quellen und Hilfsmittel verwendet habe.

Aachen, im Juni 2005